Article

Free Radical Reactions of Methionine in Peptides: Mechanisms Relevant to β-Amyloid Oxidation and Alzheimer's Disease

Christian Schneich, Dariusz Pogocki, Gordon L. Hug, and Krzysztof Bobrowski

J. Am. Chem. Soc., **2003**, 125 (45), 13700-13713• DOI: 10.1021/ja036733b • Publication Date (Web): 18 October 2003

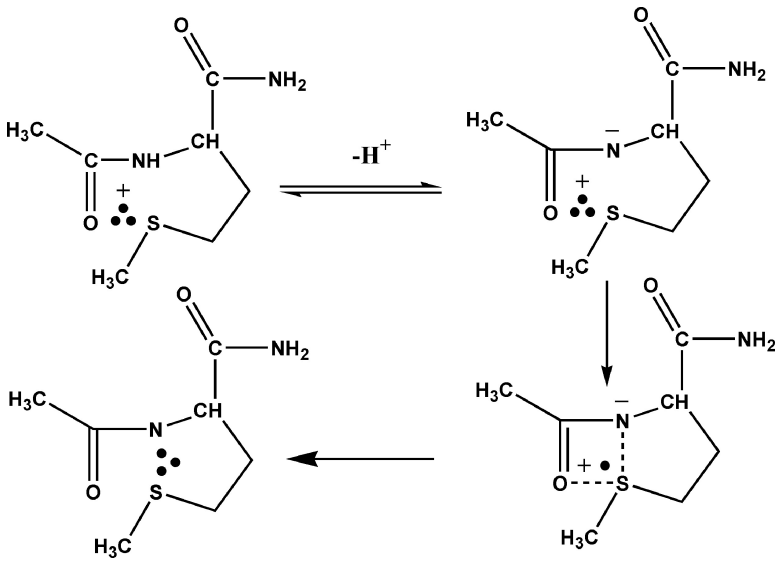

More About This Article

Additional resources and features associated with this article are available within the HTML version:

- Supporting Information
- Links to the 12 articles that cite this article, as of the time of this article download
- Access to high resolution figures
- Links to articles and content related to this article
- Copyright permission to reproduce figures and/or text from this article

View the Full Text HTML

J|A|C|S
ARTICLES
Published on Web 10/18/2003

Free Radical Reactions of Methionine in Peptides: Mechanisms Relevant to β-Amyloid Oxidation and Alzheimer's Disease

Christian Schöneich,*,† Dariusz Pogocki,‡ Gordon L. Hug,§ and Krzysztof Bobrowski*,‡

Contribution from the Department of Pharmaceutical Chemistry, University of Kansas, 2095 Constant Avenue, Lawrence, Kansas 66047; Institute of Nuclear Chemistry and Technology, Dorodna 16, 03-195 Warsaw, Poland; and Radiation Laboratory, University of Notre Dame, Notre Dame, Indiana 46556

Received June 17, 2003; E-mail: schoneic@ukans.edu

Abstract: The pathogenesis of Alzheimer's disease is strongly associated with the formation and deposition of β-amyloid peptide (βAP) in the brain. This peptide contains a methionine (Met) residue in the C-terminal domain, which is important for its neurotoxicity and its propensity to reduce transition metals and to form reactive oxygen species. Theoretical studies have proposed the formation of βAP Met radical cations as intermediates, but no experimental evidence with regard to formation and reactivity of these species in βAP is available, largely due to the insolubility of the peptide. To define the potential reactions of Met radical cations in βAP, we have performed time-resolved UV spectroscopic and conductivity studies with small model peptides, which show for the first time that (i) Met radical cations in peptides can be stabilized through bond formation with either the oxygen or the nitrogen atoms of adjacent peptide bonds; (ii) the formation of sulfur−oxygen bonds is kinetically preferred, but on longer time scales, sulfur−oxygen bonds convert into sulfur−nitrogen bonds in a pH-dependent manner; and (iii) ultimately, sulfur−nitrogen bonded radicals may transform intramolecularly into carbon-centered radicals located on the $^{\alpha}$C moiety of the peptide backbone.

Introduction

The deposition of β-amyloid peptide (βAP) into senile plaque is an important factor in the pathogenesis of Alzheimer's disease.[1−5] A hallmark of βAP is its pronounced tendency to aggregate, ultimately forming fibrils in which βAP adopts a β-sheet conformation.[8−13] For a long time, βAP aggregation has been considered the key parameter by which βAP formation influences the progression of Alzheimer's disease. However, increasing experimental evidence is mounting that aggregation may not be the only mechanism of βAP action[14−23] but that oxidative stress associated with metal-catalyzed transformations of βAP represents an important pathway of the pathology. βAP shows a high affinity to Zn^{II} and Cu^{II}, and binding of these metals promotes βAP aggregation.[8,21,24−28] Moreover, the peptide efficiently reduces Cu^{II} to Cu^{I}, a process which

† University of Kansas.
‡ Institute of Nuclear Chemistry and Technology.
§ University of Notre Dame.

(1) Selkoe, D. J. *J. Biol. Chem.* **1996**, *271*, 18295−18298.
(2) Wolfe, M. S.; De Los Angeles, J.; Miller, D. D.; Xia, W.; Selkoe, D. J. *Biochemistry* **1999**, *38*, 11223−11230.
(3) Tanzi, R. E. *J. Clin. Invest.* **1999**, *104*, 1175−1179.
(4) Xia, W.; Ray, W. J.; Ostaszewski, B. L.; Rahmati, T.; Kimberley, W. T.; Wolfe, M. S.; Zhang, J.; Goate, A. M.; Selkoe, D. J. *Proc. Natl. Acad. Sci. U.S.A.* **2000**, *97*, 9299−9304.
(5) Martin, G. M. *Exp. Gerontol.* **2000**, *35*, 439−443.
(6) Haass, C.; Koo, E. H.; Mellon, A.; Hung, A. Y.; Selkoe, D. J. *Nature* **1992**, *357*, 500−503.
(7) Seubert, P.; Vigo-Pelfrey, C.; Esch, F.; Lee, M.; Dovey, H.; Davis, D.; Sinha, S.; Schlossmacher, M.; Whaley, J.; Swindlehurst, C. *Nature* **1992**, *359*, 325−327.
(8) Bush, A. I.; Pettingell, W. H.; Multhaup, G.; d. Paradis, M.; Vonsattel, J.-P.; Gusella, J. F.; Beyreuther, K.; Masters, C. L.; Tanzi, R. E. *Science* **1994**, *265*, 1464−1467.
(9) Shen, C.-L.; Murphy, R. M. *Biophys. J.* **1995**, *69*, 640−651.
(10) Walsh, D. M.; Lomakin, A.; Benedek, G. B.; Condron, M. M.; Teplow, D. B. *J. Biol. Chem.* **1997**, *272*, 22364−22372.
(11) Tjernberg, L. O.; Callaway, D. J. E.; Tjernberg, A.; Hahne, S.; Lilliehöök, C.; Terenius, L.; Thyberg, J.; Nordstedt, C. *J. Biol. Chem.* **1999**, *274*, 12619−12625.
(12) Sipe, J. D.; Cohen, A. S. *J. Struct. Biol.* **2000**, *130*, 88−98.
(13) Kisilevski, R. *J. Struct. Biol.* **2000**, *130*, 99−108.
(14) Hensley, K.; Carney, J. M.; Mattson, M. P.; Aksenova, M.; Harris, M.; Wu, J. F.; Floyd, R. F.; Butterfield, D. A. *Proc. Natl. Acad. Sci. U.S.A.* **1994**, *91*, 3270−3274.
(15) Harris, M. E.; Hensley, K.; Butterfield, D. A.; Leedle, R. A.; Carney, J. M. *Exp. Neurol.* **1995**, *131*, 193−202.
(16) Butterfield, D. A. *Chem. Res. Toxicol.* **1997**, *10*, 495−506.
(17) Mattson, M. P.; Mark, R. J.; Furukawa, K.; Bruce, A. J. *Chem. Res. Toxicol.* **1997**, *10*, 507−517.
(18) Sayre, L. M.; Zagorski, M. G.; Surewicz, W. K.; Krafft, G. A.; Perry, G. *Chem. Res. Toxicol.* **1997**, *10*, 518−526.
(19) Huang, X.; Cuajungco, M. P.; Atwood, C. S.; Hartshorn, M. A.; Tyndall, J. D.; Hanson, G. R.; Stokes, K. C.; Leopold, M.; Multhaup, G.; Goldstein, L. E.; Scarpa, R. C.; Saunders, A. J.; Lim, J.; Moir, R. D.; Glabe, C.; Bowden, E. F.; Masters, C. L.; Fairlie, D. P.; Tanzi, R. E.; Bush, A. I. *J. Biol. Chem.* **1999**, *274*, 37111−37116.
(20) Huang, X.; Atwood, C. S.; Hartshorn, M. A.; Multhaup, G.; Goldstein, L. E.; Scarpa, R. C.; Cuajungco, M. P.; Gray, D. N.; Lim, J.; Moir, R. D.; Tanzi, R. E.; Bush, A. I. *Biochemistry* **1999**, *38*, 7609−7616.
(21) Curtain, C. C.; Ali, F.; Volitakis, I.; Cherny, R. A.; Norton, R. S.; Beyreuther, K.; Barrow, C. J.; Masters, C. L.; Bush, A. I.; Barnham, K. J. *J. Biol. Chem.* **2001**, *276*, 20466−20473.
(22) Varadarajan, S.; Yatin, S.; Aksenova, M.; Butterfield, D. A. *J. Struct. Biol.* **2000**, *130*, 184−208.
(23) Varadarajan, S.; Kanski, J.; Aksenova, M.; Lauderback, C.; Butterfield, D. A. *J. Am. Chem. Soc.* **2001**, *123*, 5625−5631.
(24) Huang, X.; Atwood, C. S.; Moir, R. D.; Hartshorn, M. A.; Vonsattel, J.-P.; Tanzi, R. E.; Bush, A. I. *J. Biol. Chem.* **1997**, *272*, 26464−26470.

10.1021/ja036733b CCC: $25.00

ultimately generates hydrogen peroxide in aerobic solution.[19−23] Importantly, Cu^{II} reduction is only observed with full length βAP, which contains (i) Cu^{II}-binding His residues in the N-terminal domain and (ii) Met^{35} in the C-terminal domain. Truncated congeners of βAP, which either lack the N-terminal His residues, for example, βAP25−35, or the Met^{35}-containing C-terminus, for example, βAP1−28, do not reduce Cu^{II}.[21,23] However, free Met can reduce Cu^{II} if incubated together with βAP1−28 and sodium dodecyl sulfate (SDS).[21]

These data point to an important role for Met^{35} in βAP as an electron donor for Cu^{II} reduction and in the initiation of oxidative stress. Stoichiometrically, the reduction of Cu^{II} to Cu^{I} requires the one-electron oxidation of Met to a Met radical cation ($MetS^{+\bullet}$) (reaction 1):

$$\mathrm{Met(S) + Cu^{II} = Met(S^{+\bullet}) + Cu^{I}} \qquad (1)$$

Electrochemical experiments reveal that $E°(Cu^{I}/Cu^{II}\beta\mathrm{AP}) \approx 0.5$ V[21] and $E_p(\mathrm{Met/MetS^{+\bullet}}) \geq 1.3$ V versus Ag/AgCl;[29] that is, equilibrium 1 is located largely on the left-hand side. However, equilibrium 1 may be shifted toward the right-hand side through (i) the efficient removal of $MetS^{+\bullet}$ (and/or Cu^{I}) via irreversible follow-up reactions or (ii) a shift of $E_p(\mathrm{Met/MetS^{+\bullet}})$ to less positive values.

The one-electron oxidation of organic sulfides is catalyzed by neighboring groups containing electron-rich heteroatoms, which stabilize the forming sulfide radical cations.[30,31] Our recent molecular modeling calculations show that in the C-terminal helical structure of βAP such stabilization is possible between the sulfide radical cation of Met^{35} and the carbonyl oxygen of the peptide bond C-terminal of Ile^{31}.[32] As evidence for this type of stabilization, we have recently reported experiments confirming sulfur−oxygen bond formation between $MetS^{+\bullet}$ and an amide carbonyl group in *N*-acetylmethionine amide (*N*-Ac-Met-NH_2) (see species **5.1** in Scheme 1).[33] *N*-Ac-Met-NH_2 represents a simple chemical model for the amino acid Met incorporated in a peptide. The reaction pathways of *N*-Ac-Met-NH_2 oxidation were characterized at pH 4.0[33] by monitoring the time development of radicals and radical ions following pulse radiolysis of aqueous solutions, coupled to time-resolved UV−vis spectroscopy and conductivity detection. All reactions are displayed in Scheme 1 ($N = 1$).

The formation of radical cations is initiated by the reaction of $^{\bullet}OH$ radicals with the thioether function of *N*-Ac-Met-NH_2, that leads to the formation of four UV/vis-detectable intermediates: hydroxysulfuranyl radical (**1.1**) (reaction 2.1), the two α-(alkylthio)alkyl radicals **3.1a** and **3.1b** (reaction 4.1), the intermolecularly sulfur−sulfur three-electron bonded dimeric radical cation **4.1** (reaction 5.1), and the *intra*molecular sulfur−oxygen bonded radical cation **5.1** (reaction 6.1).[33] The formation of radical cations **4.1** and **5.1** is paralleled by a net decrease in

Scheme 1

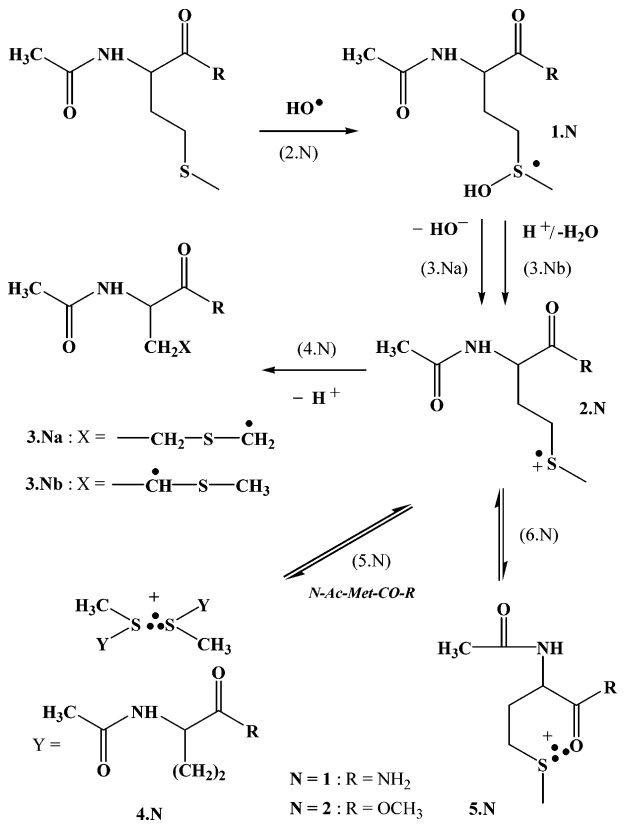

equivalent conductivity[33] through stoichiometric neutralization (reaction 7; $k_7 = 1.4 \times 10^{11}\ \mathrm{M^{-1}\ s^{-1}}$)[34] of highly conducting protons by OH^- (generated via reactions 3.1a/b).

$$\mathrm{H^+ + OH^- \rightarrow H_2O} \qquad (7)$$

In fact, this parallel decrease in net conductivity is an important experimental detail supporting radical cation formation. Hence, even in the absence of amino acids with catalytically active side chains (such as Asp, Glu, Ser, or Thr) in the C-terminal βAP domain, $A^{30}IIGLM^{35}VGGVV^{40}$, Met oxidation to $MetS^{+\bullet}$ may be assisted by the peptide bond in the backbone.

This mechanism also provides a convenient route to carbon-centered radicals from βAP (a novel pathway will be characterized in this paper). Electron spin resonance (ESR) experiments have shown the formation of βAP-derived radicals (possibly peroxyl radicals) during the decomposition of native βAP1−42 but not its Met^{35}-Nle mutant, suggesting that their formation requires Met oxidation.[22] Peroxyl radicals would form via addition of molecular oxygen to initially generated carbon-centered radicals. A simple Met-dependent route to carbon-centered radicals would be the deprotonation of $MetS^{+\bullet}$

(25) Atwood, C. S.; Moir, R. D.; Huang, X.; Scarpa, R. C.; Bacarra, N. M. E.; Romano, D. M.; Hartshorn, M. A.; Tanzi, R. E.; Bush, A. I. *J. Biol. Chem.* **1998**, *273*, 12817−12826.
(26) Atwood, C. S.; Scarpa, R. C.; Huang, X.; Moir, R. D.; Jones, W. D.; Fairlie, D. P.; Tanzi, R. E.; Bush, A. I. *J. Neurochem.* **2000**, *75*, 1219−1233.
(27) Liu, S.-T.; Howlett, G.; Barrow, C. J. *Biochemistry* **1999**, *38*, 9373−9378.
(28) Miura, T.; Suzuki, K.; Kohata, N.; Takeuchi, H. *Biochemistry* **2000**, *39*, 7024−7031.
(29) Sanaullah; Wilson, G. S.; Glass, R. S. *J. Inorg. Biochem.* **1994**, *55*, 87−99.
(30) Asmus, K.-D.; Bonifacic, M. In *S-Centered Radicals*; Alfassi, Z. B., Ed.; Wiley: New York, 1999; pp 141−191.
(31) Glass, R. S. *Top. Curr. Chem.* **1999**, *205*, 1−87.
(32) Pogocki, D.; Schöneich, Ch. *Chem. Res. Toxicol.* **2002**, *15*, 408−418.
(33) Schöneich, Ch.; Pogocki, D.; Wisniowski, P.; Hug, G. L.; Bobrowski, K. *J. Am. Chem. Soc.* **2000**, *122*, 10224−10225.
(34) Eigen, M.; De Maeyer, L. *Z. Elektrochem.* **1955**, *59*, 986.
(35) Hiller, K.-O.; Masloch, B.; Göbl, M.; Asmus, K.-D. *J. Am. Chem. Soc.* **1981**, *103*, 2734−2743.
(36) Hiller, K.-O.; Asmus, K.-D. *Int. J. Radiat. Biol.* **1981**, *40*, 597−604.
(37) Rauk, A.; Armstrong, D. A.; Fairlie, D. P. *J. Am. Chem. Soc.* **2000**, *122*, 9761−9767.
(38) Von Sonntag, C. *The Chemical Basis of Radiation Biology*; Taylor & Francis: London, 1987.
(39) Schuler, R. H.; Hartzell, A. L.; Behar, B. *J. Phys. Chem.* **1981**, *85*, 192−199.
(40) Buxton, G. V.; Greenstock, C. L.; Helman, W. P.; Ross, A. B. *J. Phys. Chem. Ref. Data* **1988**, *17*, 513−886.

(analogous to reaction 4.1 in Scheme 1);[35,36] however, theoretical calculations by Rauk and co-workers[37] propose an alternative pathway involving hydrogen transfer from an adjacent Gly residue to $MetS^{+\bullet}$. In this paper, we will provide a complete mechanistic study of the redox processes of Met in peptide models relevant to βAP oxidation. We will characterize in detail (i) the parameters controlling the anchimeric assistance of a peptide bond in the one-electron oxidation of Met to $MetS^{+\bullet}$, (ii) subsequent reactions of $MetS^{+\bullet}$, and (iii) a novel pathway for the formation of carbon-centered radicals at the $^{\alpha}$C position of Met and (iv) examine the potential reactivity of $MetS^{+\bullet}$ toward the $^{\alpha}$C−H bond of adjacent Gly residues.

Experimental Section

Materials. *N*-acetylmethionine amide (*N*-Ac-L-Met-NH_2), *N*-acetylmethionine methyl ester (*N*-Ac-L-Met-OMe), *N*-acetylalanine amide (*N*-Ac-L-Ala-NH_2) and the linear peptide L-Ala-L-Ala were purchased from Bachem (Torrance, CA). *N*-Ac-Gly-L-Met-Gly (*N*-Ac-GMG) and *N*-Ac-Gly-Gly-Gly-L-Met-Gly-Gly-Gly (*N*-Ac-GGGMGGG) were synthesized using standard solid-phase chemistry. The synthetic peptides were purified by reversed-phase HPLC, and their identity was controlled by mass spectrometry.

Radiation-Induced Chemical Processes in Water. The pulse irradiation of water leads to the formation of the primary reactive species and protons shown in reaction 8.[38]

$$H_2O \rightarrow e_{aq}^-, {}^{\bullet}H, {}^{\bullet}OH, H^+ \qquad (8)$$

In N_2O-saturated solutions ($[N_2O]_{sat} \approx 2 \times 10^{-2}$ M), the hydrated electrons, e_{aq}^-, are converted into $^{\bullet}$OH radicals according to eq 9 ($k_9 = 9.1 \times 10^9$ M^{-1} s^{-1}),[38]

$$e_{aq}^- + N_2O + H_2O \rightarrow {}^{\bullet}OH + {}^-OH + N_2 \qquad (9)$$

Reaction 9 nearly doubles the amount of $^{\bullet}$OH radicals available for reaction with substrates. The effective radiation chemical yields, *G*, of the primary species available for the reaction with a substrate depend on the concentration of the added substrate. For N_2O-saturated solutions, the effective radiation chemical yield of $^{\bullet}$OH converting a given substrate into substrate-derived radicals can be calculated on the basis of formula I given by Schuler et al.,[39] where *G* refers to the number of species generated/reacted per 100 eV absorbed energy ($G = 1.0$ corresponds to 0.1036 μM generated/reacted species per 1 J of absorbed energy; G^{N_2O} refers to *G* in N_2O-saturated solution).

$$G^{N_2O}(OH^{\bullet}) = 5.2 + 3.0\,\frac{[k_S[S]/(4.7 \times 10^8)]^{1/2}}{1 + [k_S[S]/(4.7 \times 10^8)]^{1/2}} \qquad (I)$$

The initial radiation chemical yields of $H^{\bullet}$ are on the order of $G_i(H^{\bullet}) \approx 0.6$. For practical purposes, the G unit rather than SI unit for radiation chemical yields is used.

In this paper, the added substrate(s) are two *N*-acetylmethionine derivatives and two *N*-acetylated model oligopeptides, containing methionyl and glycyl residues, at concentrations of 2×10^{-4} M. Taking a representative value of $k_S = k(^{\bullet}OH + N\text{-Ac-Met}) = 6.7 \times 10^9$ M^{-1} s^{-1},[40] we calculated the initial yields of $^{\bullet}$OH reacting with our Met-containing model peptides as $G_i(^{\bullet}OH) = 5.35$ and, therefore, $G_i(^{\bullet}OH + H^{\bullet}) = 5.95$.

Pulse Radiolysis. Pulse radiolysis experiments were performed on two different linear electron accelerators, the 8 MeV Titan Beta model TBS-8/16-1 electron accelerator at the Radiation Laboratory[41] and the 10 MeV LAE10 electron accelerator at the Institute of Nuclear Chemistry and Technology in Warsaw,[42] with typical pulse lengths of 2−10 ns and 8 ns, respectively. Absorbed doses were on the order of 3−6 Gy (1 Gy = 1 J/kg). For time-resolved measurements of optical spectra, N_2O-saturated solutions of 10^{-2} M potassium thiocyanate were used as the dosimeter, taking a radiation chemical yield of G = 6.13 and a molar extinction coefficient for $(SCN)_2^{\bullet-}$ of $\epsilon_{472} = 7580$ M^{-1} cm^{-1}.[43] For time-resolved conductivity measurements, the dosimetry was achieved using aqueous solutions saturated with CH_3Cl. Pulse irradiation yields H^+ and Cl^- with $G(H^+) = G(Cl^-) = 2.75$, according to reactions 8 and 10. The respective equivalent conductivities at 18 °C were taken as $\Lambda(H^+) = 315$ S cm^2 $equiv^{-1}$ and $\Lambda(Cl^-) = 65$ S cm^2 $equiv^{-1}$.[44]

$$e_{aq}^- + CH_3Cl \rightarrow CH_3^{\bullet} + Cl^- \qquad (10)$$

All experiments were performed with a continuous flow of the sample solutions at room temperature (~20 °C).

Deconvolution of Time-Resolved Optical Spectra. Optical spectra, monitored at various time points after pulse irradiation, were deconvoluted into specific components (representing individual transients) by linear regression according to equation II.[45]

$$G \times \epsilon(\lambda_j) = \Sigma G_i \times \epsilon_i(\lambda_j) \qquad (II)$$

Here, $G \times \epsilon(\lambda_j)$ is equal to the observed absorbance change $\Delta A(\lambda_j)$ of the composite spectrum multiplied by the factor (*F*) from the dosimetry. $F = \epsilon_{472} \times G((SCN)_2^{\bullet-})/\Delta A_{472}$, where ϵ_{472} is the molar extinction coefficient of $(SCN)^{\bullet-}$ at 472 nm, $G((SCN)_2^{\bullet-})$ is the radiation chemical yield of the $(SCN)_2^{\bullet-}$ radicals, and ΔA_{472} represents the observed absorbance change at 472 nm in the thiocyanate dosimeter. G_i is the linear regression coefficient of the *i*-th species, and $\epsilon_i(\lambda_j)$ is the molar extinction coefficient of the *i*-th species at the *j*-th wavelength of observation. Further details of this method have been described elsewhere.[46] Several criteria were applied to validate the deconvolutions and eliminate unreasonable fits. (1) Within ±15%, the combined yields of the transient species derived from their respective extinction coefficients cannot exceed the initial radiation chemical yield of primary radical species, that is, $G_i(H^{\bullet} + {}^{\bullet}OH) = 5.95$. The error limit of ±15% allows for a ±5% variation in the experimental data and a ±10% combined error in the reported extinction coefficients for the UV spectra of the components under consideration. (2) Wherever experimentally measurable, the formation of (radical) ions must be accompanied by the correct change in equivalent conductivity. (3) Based on the known formation and decomposition kinetics, an initial adduct of $^{\bullet}$OH to organic sulfides as well as the Met side chain completely decomposes within ca. 6 μs.[35,47] Therefore, deconvolutions for spectra monitored at >6 μs after pulse irradiation did not include the specific spectrum of such $^{\bullet}$OH adducts (see below). The radiation chemical yields of the respective species in the optical spectra were calculated taking the following representative extinction coefficients: ϵ_{340}(**1.N**) = 3400 M^{-1} cm^{-1},[47] ϵ_{290}(**3.Na/3.Nb**) = 3000 M^{-1} cm^{-1},[36] ϵ_{480}(**4.N**) = 6900 M^{-1} cm^{-1},[48] ϵ_{400}(**5.N**) = 3250 M^{-1} cm^{-1},[49] ϵ_{350}(**6.N**) = 3150 M^{-1} cm^{-1} (vide infra), ϵ_{390}(**7.Na/7.Nb**) = 4500 M^{-1} cm^{-1} (vide infra),[50] ϵ_{260}(**8**)

(41) Hug, G. L.; Wang, Y.; Schöneich, Ch.; Jiang, P.-Y.; Fessenden, R. W. *Radiat. Phys. Chem.* **1999**, *54*, 559−566.
(42) Mirkowski, J.; Wisniowski, P.; Bobrowski, K. *INCT Annual Report* **2000**, 31−33.
(43) Janata, E.; Schuler, R. H. *J. Phys. Chem.* **1982**, *86*, 2078−2084.
(44) (a) Asmus, K.-D. *Int. J. Radiat. Phys. Chem.* **1972**, *4*, 417−437. (b) Landolt-Börnstein *Zahlenwerte und Funktionen*; Springer-Verlag: Berlin, 1960; Vol. 7 II.
(45) Bevington, P. R. *Data Reduction and Error Analysis for the Physical Sciences*; McGraw-Hill: New York, 1969.
(46) Marciniak, B.; Bobrowski, K.; Hug, G. L. *J. Phys. Chem.* **1993**, *97*, 11937−11943.
(47) Schöneich, Ch.; Bobrowski, K. *J. Am. Chem. Soc.* **1993**, *115*, 6538−6547.
(48) Wisniowski, P. Influence of neighboring groups on radiation-induced radical processes in thioethers. Ph.D. Thesis, Institute of Nuclear Chemistry and Technology, Warsaw, 2001.
(49) Schöneich, Ch.; Zhao, F.; Madden, K. P.; Bobrowski, K. *J. Am. Chem. Soc.* **1994**, *116*, 4641−4652.

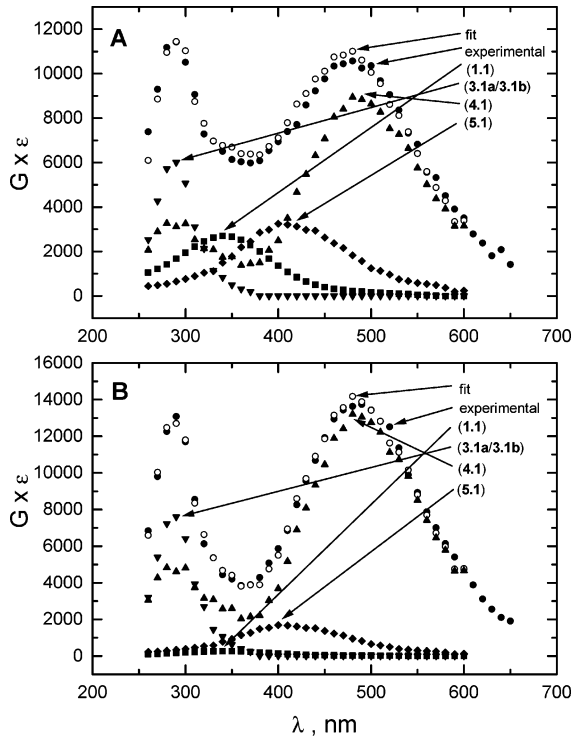

Figure 1. Resolution of the spectral components in the transient absorption spectra following the •OH-induced oxidation of *N*-acetylmethionine amide (2×10^{-4} M) in N_2O saturated aqueous solutions at pH 4.0 taken (A) 2 μs and (B) 4 μs after the pulse.

$= 13\,000$ M^{-1} cm^{-1} (vide infra) and $\epsilon_{350}(\mathbf{8}) = 3700$ M^{-1} cm^{-1} (vide infra).

Results

***N*-Acetylmethionine Amide (*N*-Ac-Met-NH_2).** We extended our previous optical and conductivity pulse radiolysis studies at pH 4.0[33] to additional time points and expanded the pH region up to pH 5.40 (conductivity experiments at pH values much larger than 5.4 are difficult to interpret due to the slow rate for neutralization reaction 7 at such pH values).

Spectrophotometric and Conductivity Detection at pH 4. Figure 1 parts A and B display the experimental optical spectra (closed circles) recorded at 2 and 4 μs after pulse irradiation of N_2O-saturated aqueous solutions, pH 4.0, of 2×10^{-4} M *N*-Ac-Met-NH_2. They can be deconvoluted into contributions from the following components (see Scheme 1, $N = 1$): hydroxysulfuranyl radical **1.1**, the two α-(alkylthio)alkyl radicals **3.1a** and **3.1b**, the intermolecularly sulfur−sulfur three-electron bonded dimeric radical cation **4.1**, and the intramolecular sulfur−oxygen bonded radical cation **5.1**.

At 2 μs after the pulse, the sum over all component spectra with their respective yields (Table S1, entry 1; Tables S1−S4 are available as Supporting Information) results in an excellent fit (open circles) of the experimental spectra (Figure 1A). Radical cations **4.1** and **5.1** are present with yields of $G_{\mathbf{4.1}} = 1.5$ and $G_{\mathbf{5.1}} = 1.2$ ($G_{\mathbf{4.1}+\mathbf{5.1}} = 2.7$), confirmed by time-resolved conductivity experiments, which yield G(ions) = 2.7 according to the following calculation: the net decrease in equivalent conductivity results from stoichiometric neutralization of highly conducting protons ($\Lambda = 315$ S cm^2 $equiv^{-1}$ [44]) by OH^- (generated via reactions 3.1a/b), and parallel formation of sulfide radical cations ($\Lambda \approx 45$ S cm^2 $equiv^{-1}$ [51]). Thus, the overall loss of equivalent conductivity is calculated as $\Delta\Lambda = +45 - 315 = -270$ S cm^2 $equiv^{-1}$. Division of the experimental change of equivalent conductivity, $G \times \Delta\Lambda = -730$ S cm^2 (Figure 2A) (corrected for small contributions of $O_2^{\bullet -}$[52]) by $\Delta\Lambda = -270$ S cm^2 $equiv^{-1}$ yields $G = 2.7$ for sulfide radical cations **4.1** and/or **5.1** at 2 μs after the pulse.

At this point, it is important to note that the higher yields of **4.1** compared to **5.1** are solely due to the experimental *N*-Ac-Met-NH_2 concentration of 2×10^{-4} M. Lower, physiologically relevant, concentrations of the peptide would certainly favor the intramolecular species **5.1** over the intermolecular intermediate **4.1**. However, the experimental concentration of 2×10^{-4} M represents the lower practical limit, as otherwise the formation rate of **1.1** would significantly overlap with its decomposition.

At 4 μs after the pulse (Figure 1B), the combined yield of **4.1** and **5.1**, $G_{\mathbf{4.1}+\mathbf{5.1}} = 2.9$ (Table S1, entry 2), shows some deviation from G(ions). Division of the experimental change in equivalent conductivity, $G \times \Delta\Lambda = -650$ S cm^2 (corrected for small contributions of $O_2^{\bullet -}$[52]) by $\Delta\Lambda = -270$ S cm^2 $equiv^{-1}$ yields G(ions) = 2.4. This important observation will be discussed later (vide infra: ***N*-acetylmethionine methyl ester**). At 8 μs (Table S1, entry 4) and 15 μs (Table S1, entry 5) after the pulse, the fits of the experimental spectra require only contributions from two components: **3.1a/3.1b** and the radical cation **4.1** (with $G_{\mathbf{4.1}} = 2.1$ and 1.8 at 8 μs and 15 μs, respectively). At these times after the pulse, the corrected[52] negative conductivity signals reach $(G \times \Delta\Lambda)_{corr} = -540$ S cm^2 and −460 S cm^2 at 8 μs and 15 μs, respectively, yielding G(ions) = 2.0 and 1.7, which are in very good agreement with the respective $G_{\mathbf{4.1}}$ quantified by optical spectroscopy.

Conductivity Detection at pH 4.0−5.4. Figure 2 displays conductivity versus time plots recorded for pH 4.0, 4.6, 5.0, and 5.4. They show decreasing amplitudes of negative conductivity with increasing pH with the following pH-dependent maximal losses of net conductivity observed at the following times after pulse irradiation: for pH 4.0, $G \times \Delta\Lambda = -730$ S cm^2 at 2.0 μs (Figure 2A); for pH 4.6, $G \times \Delta\Lambda = -520$ S cm^2 at 3.0 μs (Figure 2B); for pH 5.0, $G \times \Delta\Lambda = -350$ S cm^2 at 6 μs (Figure 2C); and for pH 5.4, $G \times \Delta\Lambda = -270$ S cm^2 at 10 μs after the pulse (Figure 2D). The different times to reach the maximal net loss are caused by the different proton concentrations available for reactions 3.1a/7 and 3.1b (Scheme 1). Correction for some superoxide formation[52] yields the following $(G \times \Delta\Lambda)_{corr}$: −730 S cm^2 (pH 4.0), −570 S cm^2 (pH 4.6), −420 S cm^2 (pH 5.0), and −375 S cm^2 (pH 5.40). The different maximal net losses of equivalent conductivity

(50) Pogocki, D. Ph.D. Thesis, Institute of Nuclear Chemistry and Technology, Warsaw, Poland, 1996.

(51) Steffen, L. K.; Glass, R. S.; Sabahi, M.; Wilson, G. S.; Schöneich, Ch.; Mahling, S.; Asmus, K.-D. *J. Am. Chem. Soc.* **1991**, *113*, 2141−2145.

(52) N_2O-saturated aqueous solutions contain micromolar concentrations of residual O_2. Based on the rate constants for the reaction of H• radicals with Met ($k = 3.5 \times 10^8$ M^{-1} s^{-1}) and O_2 ($k = 2.1 \times 10^{10}$ M^{-1} s^{-1}),[40] representative concentration of 5 μM residual O_2, and a 2.0×10^{-4} M Met-containing peptide, we calculate that ca. 60% of the H• radicals ($G = 0.36$) will react with O_2 to yield HO_2• which exists in equilibrium $HO_2^{\bullet} = H^+ + O_2^{\bullet -}$ with $pK_a = 4.8$.[53] Taking $\Lambda(H^+) = 315$ S cm^2 $equiv^{-1}$ [44] and $\Lambda(O_2^{\bullet -}) = 60$ S cm^2 $equiv^{-1}$,[54] this process yields a maximum positive change of equivalent conductivity of $G \times \Delta\Lambda = 0.36 \times 380$ $Scm^2 = 137$ Scm^2 for full dissociation of HO_2• into H^+ and $O_2^{\bullet -}$. The extent of HO_2• dissociation is pH dependent so that the actual radiation chemical yield $G(H^+/O_2^{\bullet -}) = 0.36(1 + 10^{pK_a - pH})^{-1}$. Therefore, especially the low changes of equivalent conductivity at pH > 5.0 have to be corrected for the reaction of H• radicals with O_2 while this process has a negligible effect on the yields at pH 4.0. We have validated this correction experimentally through pulse irradiation of N_2O-saturated water at defined pH values.

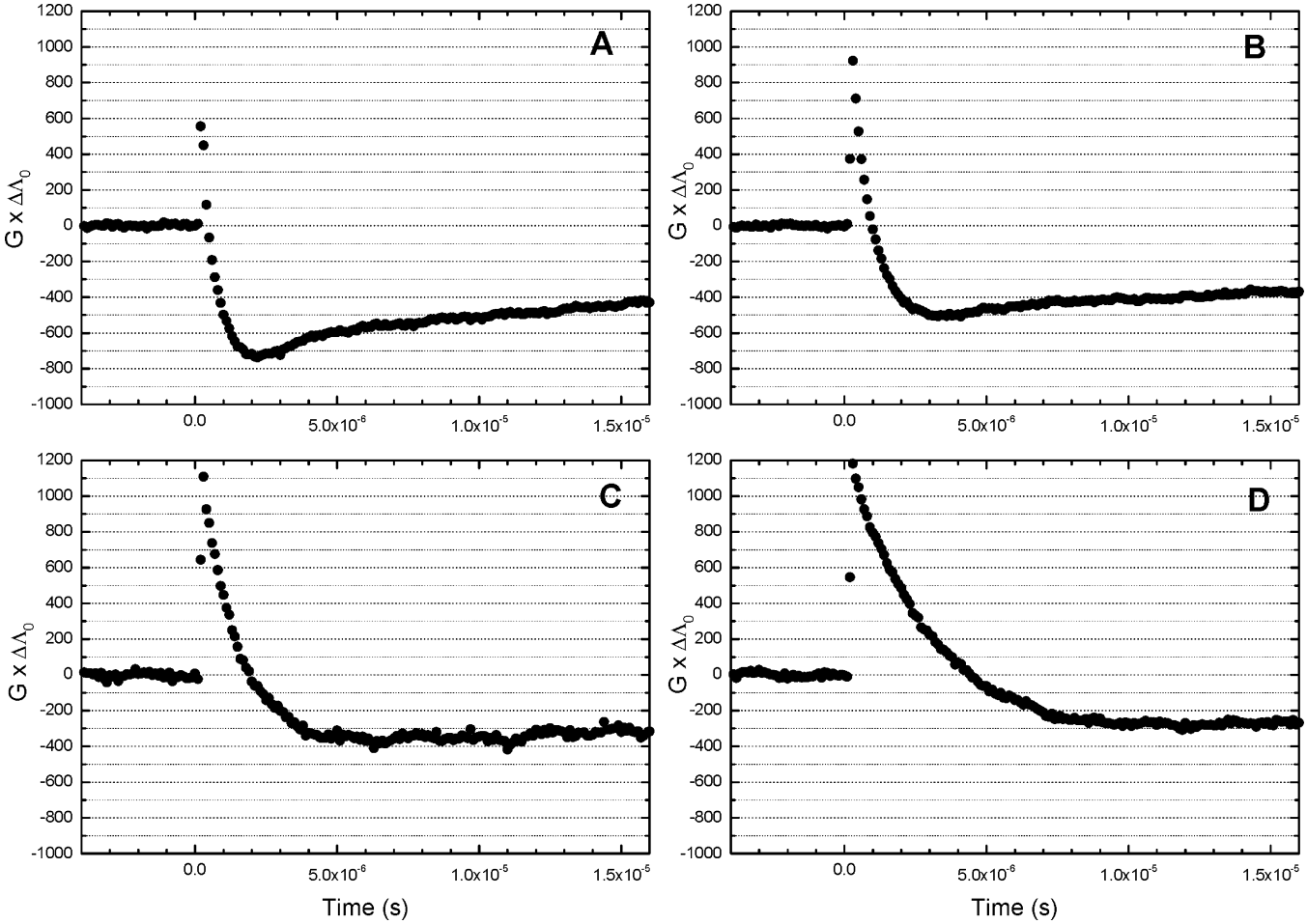

Figure 2. Equivalent conductivity changes represented as ($G \times \Delta\Lambda$) vs time profile following the •OH-induced oxidation of *N*-acetylmethionine amide (2×10^{-4} M) in N_2O saturated aqueous solutions at the following pH's: (A) 4.0, (B) 4.6, (C) 5.0, and (D) 5.4.

indicate a pH-dependent change in the yields of radical cations **4.1** and **5.1**. Division of $(G \times \Delta\Lambda)_{corr}$ by $\Delta\Lambda = -270$ S cm^2 equiv^{-1} yields G(ions) = 2.7, 2.1, 1.6, and 1.4 for pH 4.0, 4.6, 5.0, and 5.4, respectively (Table S1, entries 1, 6−8, 22, and 23).

Spectrophotometric Detection at pH 4.6−5.4. For better clarity, we will present our data in the following sequence: pH 5.4, 5.0, and 4.6.

A. pH 5.4. Figure 3A shows a yield versus time plot for the intermediates **1.1**, **3.1a**, **3.1b**, **4.1**, and **5.1** together with the total yield of all species. The total yield of all radical intermediates, $G = 6.0$ (open circles), agrees well the initial yield of primary radicals, G_i(HO•+H•) = 5.95. The apparent biphasic decay of **1.1** (closed squares) needs some discussion. Hydroxysulfuranyl radicals usually decompose with rate constants on the order of $\geq 10^6$ s^{-1}.[47,55] Therefore, the second part of the biphasic decay, present after 6 μs, cannot be due to species **1.1** but indicates the presence of an additional species with similar absorbance characteristics. The C_α radicals of amino acids or peptides of the general structure X−CO−NH−C•(R)−CO−NH−Y (**6**) display an absorption in the 300−350 nm. region.[56] Therefore, we hypothesized that the slower decay of the **1.1** component present after 6 μs following the pulse (Figure 3A) may indicate the presence of the C_α-centered radical of the Met residue in *N*-Ac-Met-NH$_2$ (radical **6.1** with R = $CH_2CH_2SCH_3$, X = CH_3, and Y = H). For quantitative analysis, we generated reference spectra for alkyl-substituted C_α-radicals by pulse radiolysis of *N*-Ac-L-Ala-NH$_2$ and L-Ala-L-Ala which show a clean absorbance peaking at $\lambda_{max} = 350$ nm with $\epsilon_{350} = 3150$ M^{-1} cm^{-1} (vide infra: ***N*-Ac-L-Ala-NH$_2$ and L-Ala-L-Ala**). This spectrum was used instead of that from **1.1** in deconvolutions of absorbance spectra at times ≥6 μs after pulse irradiation. From here on, the **6**-type radicals will be referred to as **6.N** (N = 1−4) for the following substrates: *N*-Ac-Met-NH$_2$ (N = 1), *N*-Ac-Met-OMe (N = 2), *N*-Ac-Gly-Met-Gly (N = 3), and *N*-Ac-(Gly)$_3$Met(Gly)$_3$ (N = 4).

Figure 3B shows the optical spectrum recorded at 10 μs after pulse irradiation (time point of maximal loss of equivalent conductivity at pH 5.4; see Figure 2D) of an N_2O-saturated aqueous solution of 2×10^{-4} M *N*-Ac-Met-NH$_2$ at pH 5.4, together with a spectral deconvolution into the contributions of the individual intermediates.

An excellent spectral deconvolution is achieved using the intermediates **3.1a**/**3.1b**, **4.1**, **5.1**, and **6.1** with the respective yields given in Table S1, entry 22. However, in contrast to pH 4.0, the yield of sulfur radical cations, $G_{4.1 + 5.1} = 2.6$, does not match G(ions) = 1.4, determined by conductivity measurements. A similar picture is obtained at 15 μs after the pulse, where

(53) Bielski, B. H. J.; Cabelli, D. E. *Int. J. Radiat. Biol.* **1991**, *59*, 291−319.
(54) Schuchmann, M. N.; Schuchmann, H.-P.; von Sonntag, C. *J. Am. Chem. Soc.* **1990**, *112*, 403−407.
(55) Bobrowski, K.; Pogocki, D.; Schöneich, Ch. *J. Phys. Chem. A* **1998**, *102*, 10512−10521.

$G_{4.1\ +\ 5.1}$ = 2.4 and G(ions) = 1.4 (Table S1, entry 24). Although, at both time points, $G_{4.1}$ and $G_{5.1}$ (Table S1, entries 22 and 24) are separately very close to G(ions), it is not possible to eliminate **4.1** from the spectral mix without adversely effecting the quality of the fit in the long-wavelength region of the transient spectrum. On the other hand, alternative species exist that could contribute to the optical absorption in the spectral region where **5.1** absorbs; yet these species do not contribute further to conductivity changes. In particular, sulfur−nitrogen bonded species have been observed for radical cations of a variety of amino-substituted organic sulfides[57] including *N*-methionyl peptides.[58,59] A representative spectrum taken from the pulse radiolysis data of methionine amide (Met-NH_2)[50] shows a broad absorption with λ_{max} ca. 390 nm and $\epsilon_{390} = 4500$ M^{-1} cm^{-1}.[50] Therefore, we believe that the absorption around 390−400 nm at ≥10 μs after pulse irradiation in Figure 3B may indicate the formation of a new, sulfur−nitrogen bonded intermediate of *N*-Ac-Met-NH_2, species **7.1a**/**7.1b**.

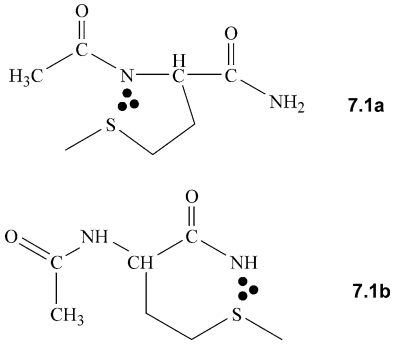

Based on the conductivity results, the sulfur−nitrogen bonded species **7.1a**/**7.1b** cannot be a radical cation, and we conclude that it is formed after the deprotonation of one of the amide functions in **2.1** (reaction 11) (for more details, see Discussion).

$$\mathbf{2.1} \rightarrow H^+ + \mathbf{7.1a/7.1b} \qquad (11)$$

The proton generated in reaction 11 replaces the proton consumed in reaction sequence 3.1a/3.1b and 7, and, therefore, the formation of **7.1a**/**7.1b** is not associated with any net change in conductivity. An excellent spectral deconvolution is now achieved when sulfur−oxygen bonded intermediate **5.1** is replaced by the sulfur−nitrogen bonded intermediate **7.1a/7.1b**. At 10 μs after the pulse, the deconvoluted experimental spectrum contains species **3.1a/3.1b**, **4.1**, **6.1**, and **7.1a/7.1b** (Figure 3C; Table S1, entry 23). This deconvolution is validated by satisfying the requirement that $G_{4.1} = G$(ions) = 1.4, consistent with the neutral character of species **7.1a/7.1b** (vide supra) (we note that, at 10 μs after the pulse, the total yield of all species is usually already smaller than $G_i(HO^\bullet + H^\bullet)$ due to the progression of radical−radical reactions). A similar deconvolution is obtained at 15 μs after the pulse (Table S1, entry 25).

Even though **5.1** and **7.1a/7.1b** have similar spectral shapes, we must note that two features allow for the discrimination between them, (i) the conductivity results and (ii) the overall yield of radical intermediates, especially at early time points after pulse irradiation: species **5.1** is a radical cation, whereas **7.1a/7.1b** is not; the molar extinction coefficient of **5.1** is ca. 33% smaller compared to that of **7.1a/7.1b**. Therefore, deconvolutions using the wrong intermediate may lead to significant deviations of the experimental G_{total} from the theoretical $G_i(HO^\bullet + H^\bullet)$.

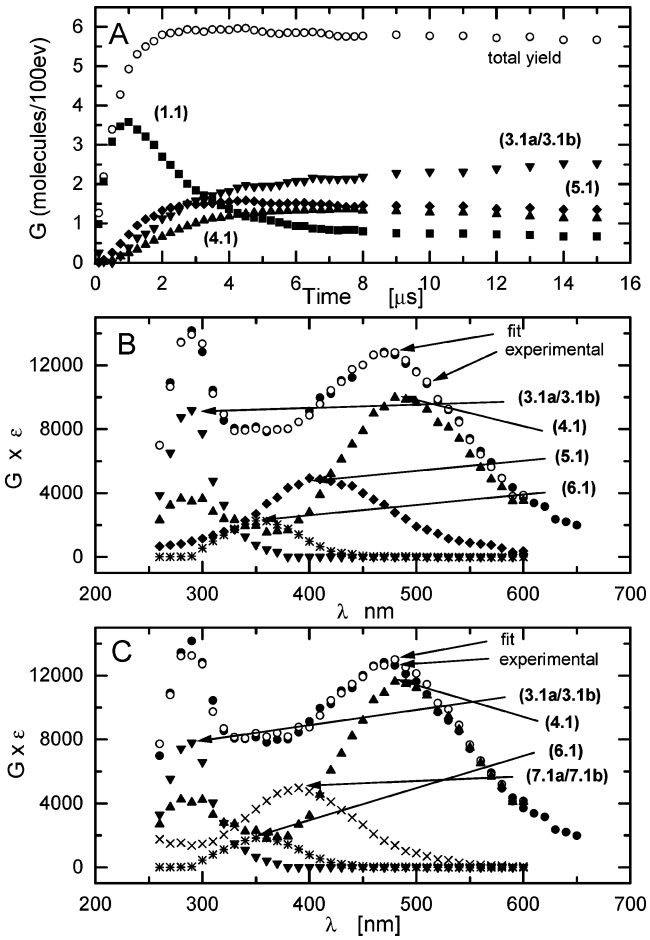

Figure 3. (A) Radiation chemical yield vs time profile for intermediates obtained after pulse radiolysis of an N_2O-saturated aqueous solution, containing 2×10^{-4} M *N*-acetyl-methionine amide at pH 5.4; (B and C) resolution of the spectral components in the transient absorption spectrum following the $^\bullet$OH-induced oxidation of *N*-acetyl-methionine amide (2×10^{-4} M) in N_2O-saturated aqueous solutions at pH 5.4 taken 10 μs after the pulse (explanation in the text).

B. pH 5.0. The optical spectrum recorded at 6 μs after pulse irradiation (time point of maximal loss of equivalent conductivity at pH 5.0; see Figure 2C) is best deconvoluted into contributions from species **1.1**, **3.1a/3.1b**, **4.1**, and both **5.1** and **7.1a/7.1b** (Figure 4; Table S1, entry 16). Neither the omission of species **7.1a**/**7.1b** (Table S1, entry 14) nor the omission of species **5.1** (Table S1, entry 15) results in a satisfactory agreement between the optically and conductometrically determined yields of radical cations. On the other hand, inclusion of both species **5.1** and **7.1a**/**7.1b** (Table S1, entry 16) provides a perfect match between G(ions) = 1.6 and $G_{4.1+5.1} = 1.6$ while significant yields of **7.1a**/**7.1b** are formed.

A similarly satisfactory deconvolution is obtained at 15 μs after the pulse taking into account the simultaneous formation of **5.1** and **7.1a/7.1b** (Table S1, entry 19).

C. pH 4.6. The optical spectrum recorded 3 μs after pulse irradiation (time point of maximal loss of equivalent conductivity at pH 4.6; see Figure 2B) is well deconvoluted into contributions from species **1.1**, **3.1a/3.1b**, **4.1**, **5.1**, and **7.1a/7.1b** (Table S1, entry 8; Figure 5A). Importantly, at this pH value, the yields of

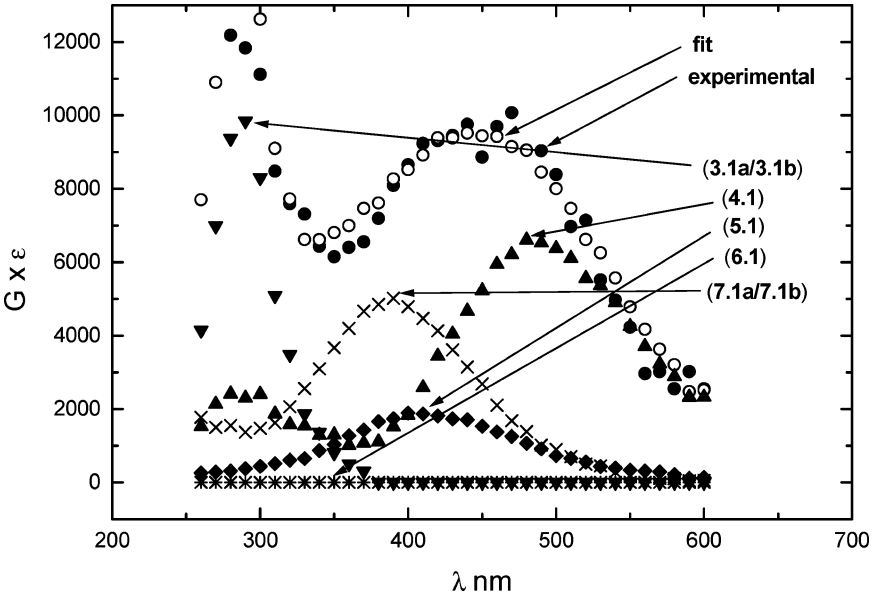

Figure 4. Resolution of the spectral components in the transient absorption spectrum following the •OH-induced oxidation of *N*-acetyl-methionine amide (2×10^{-4} M) in N_2O-saturated aqueous solutions at pH 5.0 taken 6 μs after the pulse.

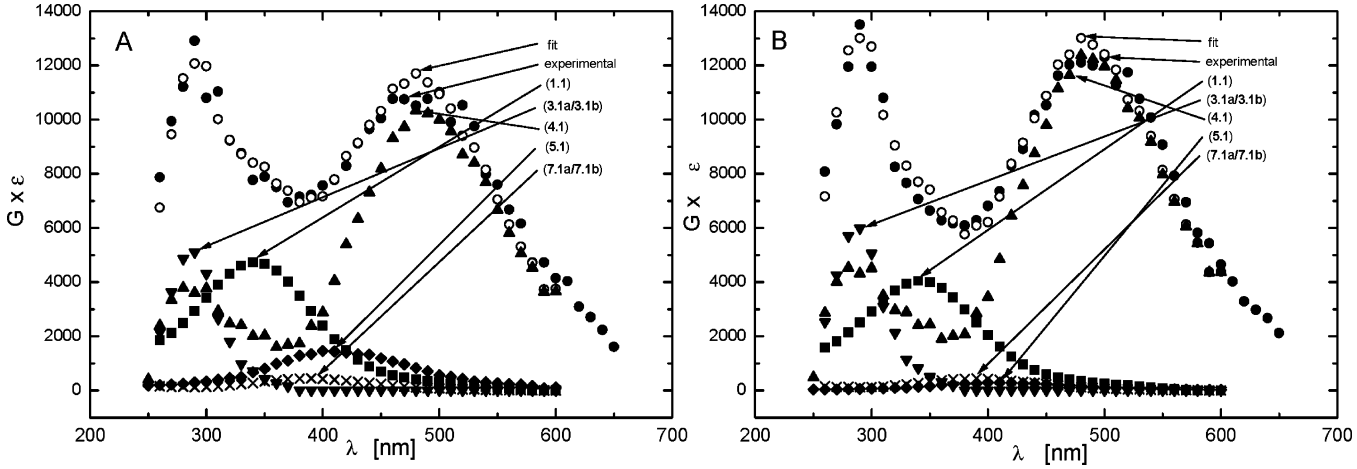

Figure 5. Resolution of the spectral components in the transient absorption spectra following the •OH-induced oxidation of *N*-acetyl-methionine amide (2×10^{-4} M) in N_2O-saturated aqueous solutions at pH 4.6 taken (A) 3 μs and (B) 4 μs after the pulse.

7.1a/**7.1b** are quite small but parallel conductivity experiments require significant yields of species **5.1** in addition to **4.1**. Similar characteristics are observed at 4 μs after the pulse (Table S1, entry 11).

***N*-Acetylmethionine Methyl Ester (*N*-Ac-Met-OMe).** In structures **7.1a** and **7.1b**, the sulfide radical cation of *N*-Ac-Met-NH_2 associates with the deprotonated amide nitrogen localized either N- or C-terminally to Met. Mechanistically, the association with the C-terminal amide nitrogen (**7.1b**) would be easy to rationalize by a stepwise process involving first S−O bond formation, followed by amide deprotonation and O-to-N migration of the sulfide radical cation (see Discussion, Scheme 4). Both the initial S−O and the final S−N bonds represent thermodynamically favorable six-membered rings. In contrast, an initial N-terminal S−O bond would involve a seven-membered ring (see Discussion, Scheme 5) prior to the formation of a five-membered S−N bond (**7.1a**). The feasibility of this reaction that leads to **7.1a** was tested with *N*-Ac-Met-OMe, that is, a Met derivative lacking the C-terminal amide, where only the possibility for N-terminal S−N bond formation exists (for *N*-Ac-Met-OMe, structure **7.2a**). The reactions of *N*-Ac-Met-OMe are shown in Scheme 1 ($N = 2$).

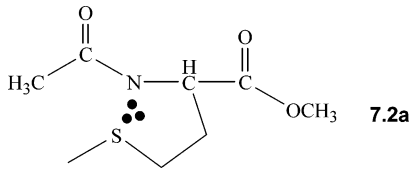

7.2a

Conductivity Detection at pH 4.0−5.7. Time-resolved conductivity experiments with *N*-Ac-Met-OMe show the following maximal pH-dependent net loss of equivalent conductivity at the following times after pulse irradiation of an N_2O-saturated aqueous solution of 2×10^{-4} M *N*-Ac-Met-OMe: for pH 4.0, $G \times \Delta\Lambda = -630$ S cm^2 at 2.0 μs (Figure 6A); pH 4.6, $G \times \Delta\Lambda = -460$ S cm^2 at 3.0 μs (Figure 6B); for pH 5.0, $G \times \Delta\Lambda = -350$ S cm^2 at 6 μs (Figure 6C); and for pH 5.7, $G \times \Delta\Lambda = -70$ S cm^2 at 40 μs after the pulse (Figure 6D).

Correction for some superoxide formation by the reaction of H-atoms with O_2[52] yields the following values for ($G \times$

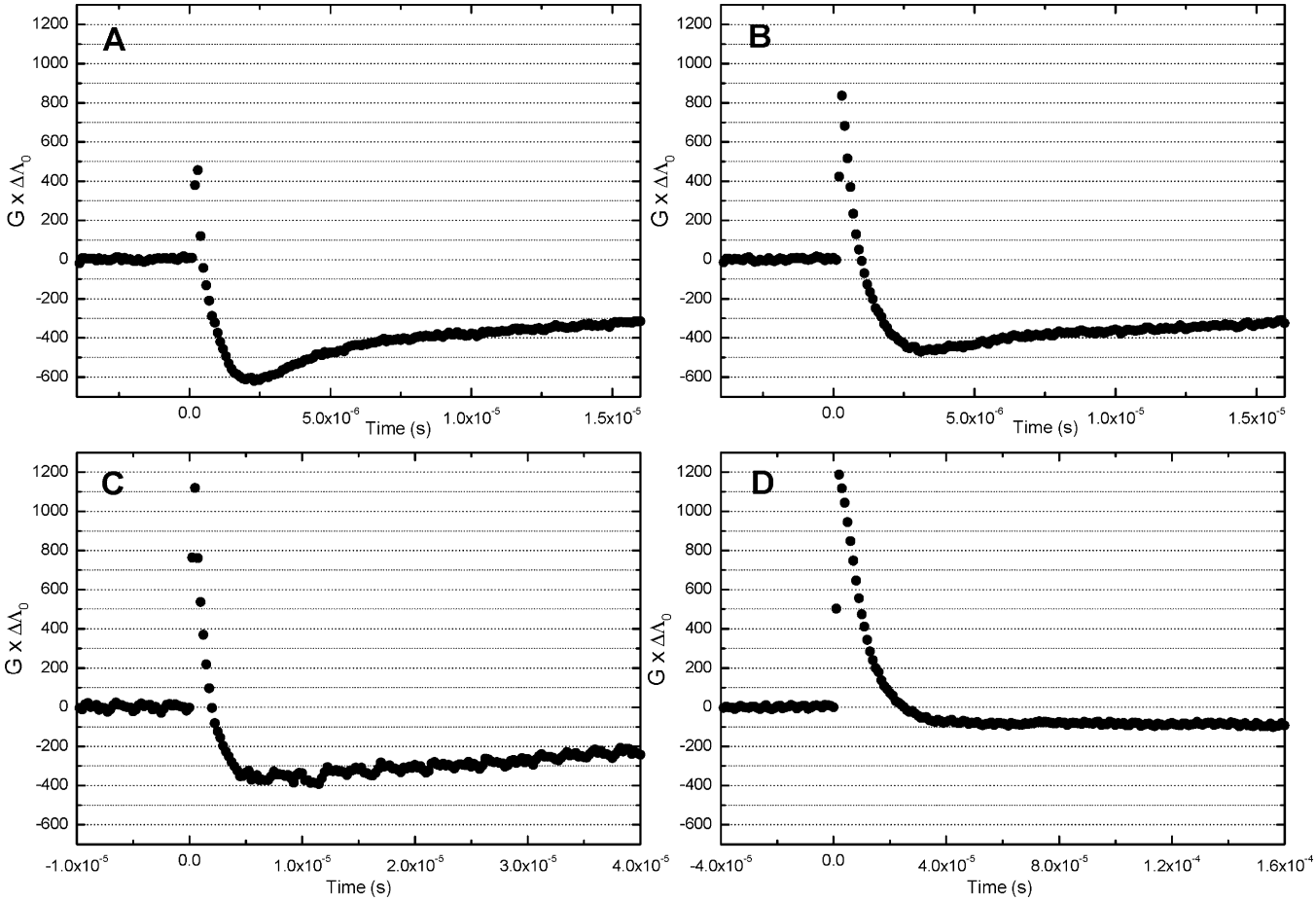

Figure 6. Equivalent conductivity changes represented as ($G \times \Delta\Lambda$) vs time profile following the •OH-induced oxidation of *N*-acetylmethionine methyl ester (2×10^{-4} M) in N_2O saturated aqueous solutions at the following pH's: (A) 4.0, (B) 4.6, (C) 5.0, and (D) 5.7.

$\Delta\Lambda)_{corr}$: -650 S cm^2 (pH 4.0), -510 S cm^2 (pH 4.6), -430 S cm^2 (pH 5.0), and -190 S cm^2 (pH 5.7). The different maximum loss of equivalent conductivity indicates a pH-dependent change in the yields of radical cations (**4.2** and **5.2**). Division of $(G \times \Delta\Lambda)_{corr}$ by $\Delta\Lambda = -270$ S cm^2 equiv^{-1} yields G(ions) = 2.4, 1.9, 1.6, and 0.7 for sulfide radical cations **4.2** and/or **5.2** at pH 4.0, 4.6, 5.0, and 5.7, respectively. These yields are very comparable to those from *N*-Ac-Met-NH_2.

This pH-dependent change in the yields of radical cations from *N*-Ac-Met-OMe would suggest that deprotonation followed by S−N bond formation is generally possible with the peptide bond N-terminal of the Met residue. This was confirmed by time-resolved optical spectroscopy (see below).

Spectrophotometric Detection at pH 4.0−5.7. A. pH 4.0. The optical spectrum recorded 2 μs after pulse irradiation (time point of maximal loss of equivalent conductivity; see Figure 6A) is well deconvoluted into contributions from species **1.2**, **3.2a**/**3.2b**, **4.2**, and **5.2** (Table S2, entry 1). The total yield of radical cations, $G_{4.2+5.2} = 2.6$, is in a fairly good agreement with G(ions) = 2.4. On the other hand, omission of species **5.2** yields a significant discrepancy between G(ions) = 2.4 and $G_{4.2}$ = 1.8 (Table S2, entry 2). Best results are obtained when deconvolutions take into account the simultaneous formation of **5.2** and **7.2a** (Table S2, entry 3), yielding a perfect match between G(ions) = $G_{4.2+5.2}$ = 2.4. In this respect, it is important to note that generally the absorption characteristics of S−O bonds are rather insensitive to the origin of the oxygen; that is, the spectra are similarly independent of the oxygen being provided by a hydroxy, carboxylate, or amide function.[33,55,60] Hence, we expect that the absorption characteristics of **5.2** are similar to those of **5.1**.

Importantly, at 4 μs after the pulse species, **5.2** is replaced by species **7.2a**, which is evident from the deconvolution in Figure 7A and the agreement between G(ions) = 2.1 and $G_{4.2}$ = 2.1 (Table S2, entry 5). With this in mind, we can now rationalize also the deconvolutions for *N*-Ac-Met-NH_2 obtained at 4 μs after pulse irradiation (Table S1, entry 3; Figure 7B). Here, a fraction of species **5.1** is replaced by **7.1a**/**7.1b**, resulting in a good agreement between G(ions) = $G_{4.1+5.1}$ = 2.4.

B. pH 4.6. An excellent deconvolution of the experimental spectrum recorded 3 μs after the pulse (time point of maximal loss of equivalent conductivity; see Figure 6B) requires the inclusion of species **4.2**, **5.2**, and **7.2a** (Table 2, entry 10). Species **7.2a** cannot be omitted (Table S2, entry 8) since this results in $G_{4.2+5.2} \gg G$(ions). On the other hand, omission of **5.2** still yields acceptable results (Table S2, entry 9). Similar considerations apply to spectra recorded at 4 and 8 μs after the pulse (see Table S2).

C. pH 5.0. The optical spectrum recorded 6 μs after pulse irradiation (time point of maximal loss of equivalent conductiv-

(56) Simic, M.; Neta, P.; Hayon, E. *J. Am. Chem. Soc.* **1970**, *92*, 4763−4768.
(57) Asmus, K.-D.; Göbl, M.; Hiller, K.-O.; Mahling, S.; Mönig, J. *J. Chem. Soc., Perkin Trans. 2* **1985**, 641−646.
(58) Bobrowski, K.; Holcman, J. *Int. J. Radiat. Biol.* **1987**, *52*, 139−144.
(59) Bobrowski, K.; Holcman, J. *J. Phys. Chem.* **1989**, *93*, 6381−6387.
(60) Bobrowski, K.; Hug, G. L.; Marciniak, B.; Miller, B.; Schöneich, Ch. *J. Am. Chem. Soc.* **1997**, *119*, 8000−8011.

Scheme 2

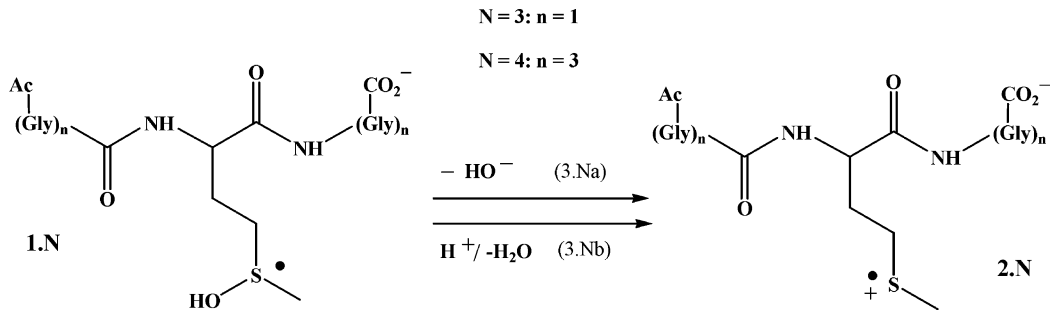

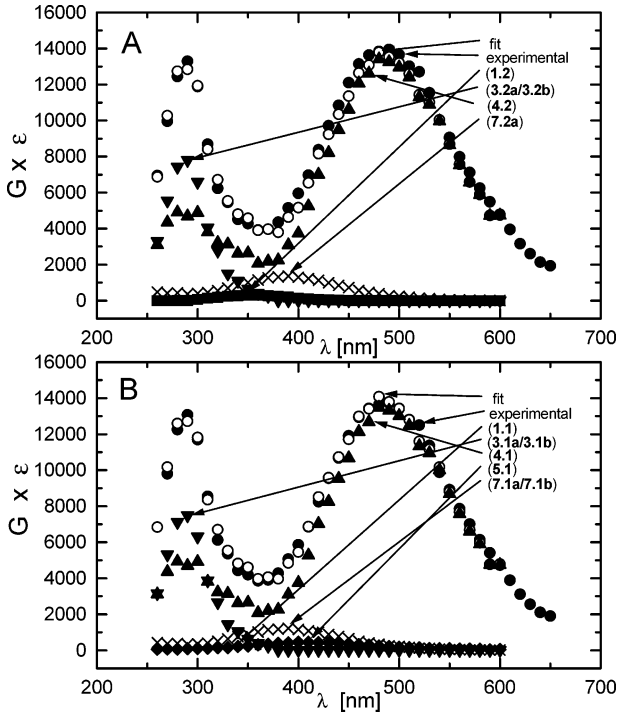

Figure 7. Resolution of the spectral components in the transient absorption spectra following the •OH-induced oxidation in N_2O-saturated aqueous solutions at pH 4.0 taken 4 μs after the pulse in (A) *N*-acetylmethionine methyl ester (2×10^{-4} M) and (B) *N*-acetylmethionine amide (2×10^{-4} M).

ity, see Figure 6C) requires the presence of both species **4.2** and **7.2a** (Table S2, entry 16) while replacement of **7.2a** by **5.2** would lead to an unacceptable mismatch between $G_{4.2+5.2} = 2.5$ and $G(\text{ions}) = 1.6$ (Table S2, entry 14).

D. pH 5.7. Figure 8 shows excellent deconvolution of the optical spectra recorded at 40 μs after pulse irradiation of an N_2O-saturated aqueous solution, pH 5.7, containing 2×10^{-4} M *N*-Ac-Met-OMe. However, to obtain the agreement between G(ions) and $G_{4.2}$ (Table S2, entry 19) deconvolution requires the presence of **7.2a** (Figure 8B) instead of **5.2a** (Figure 8A).

A preliminary conclusion can be drawn from our data on *N*-Ac-Met-NH_2 and *N*-Ac-Met-OMe. It is that there is a progressive replacement of species **5.N** by **7.Na/7.Nb** with increasing times after pulse irradiation and increasing pH. This observation suggests that species **5.N** is kinetically preferred, followed by a pH-dependent, slower conversion into **7.Na/7.Nb**.

***N*-Acetylglycyl-methionyl-glycine (*N*-Ac-Gly-Met-Gly).** Scheme 2 ($N = 3$, n=1) displays the hydroxysulfuranyl radical of *N*-Ac-Gly-Met-Gly (**1.3**) and its decomposition into the intermediary sulfide radical cation **2.3**, while Scheme 3 summarizes the potential reactions of **2.3**.

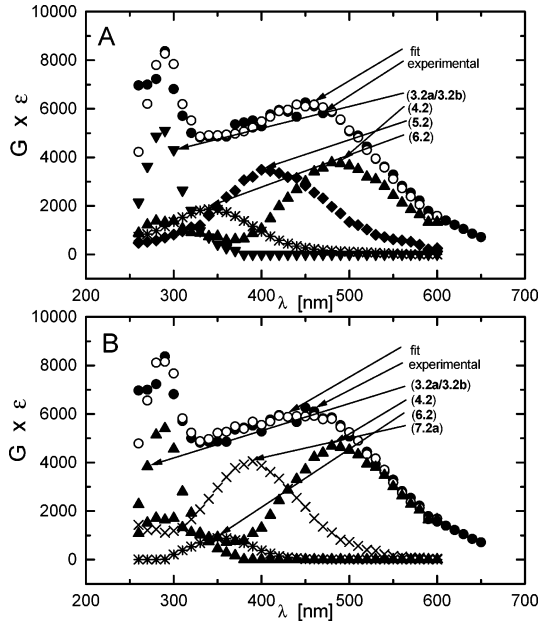

Figure 8. (A and B) Resolution of the spectral components in the transient absorption spectrum following the •OH-induced oxidation of *N*-acetylmethionine methyl ester (2×10^{-4} M) in N_2O-saturated aqueous solutions at pH 5.7 taken 40 μs after the pulse (explanation in the text).

For a quantitative analysis, we need to consider that ca. 10% of the initial HO• radicals will directly abstract H-atoms from Gly to yield the glycyl radical **8** (reaction 12).

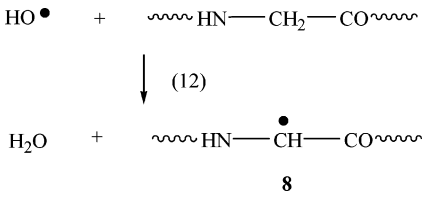

The calculated value of 10% is based on parallel reactions with $k(\text{•OH} + N\text{-Ac-Gly-Gly}) = 7.8 \times 10^8$ M^{-1} s^{-1} [40] and $k(\text{•OH} + N\text{-Ac-Met}) = 6.7 \times 10^9$ M^{-1} s^{-1}.[40] The spectrum of the resultant glycyl radical is characterized by two absorption bands peaking at 260 and 320 nm, respectively ($\epsilon_{260} = 13\,000$ M^{-1} cm^{-1}; $\epsilon_{320} = 3700$ M^{-1} cm^{-1}).[56] By analogy with the sulfur−nitrogen bonded transients derived from *N*-Ac-Met-NH_2 (**7.1a/7.1b**), the respective transients formed from *N*-Ac-GMG ($N = 3$) are depicted as structures **7.3a**/**7.3b** (Scheme 3). Figure 9A displays a conductivity versus time plot for pulse irradiation of N_2O-saturated aqueous solutions, pH 5.45, containing 2×10^{-4} M *N*-Ac-Gly-Met-Gly. A maximal loss of equivalent conductivity ($G \times \Delta\Lambda = -80$ S cm^2) is observed at 20 μs after the pulse. Correction for a small fraction of superoxide

Scheme 3

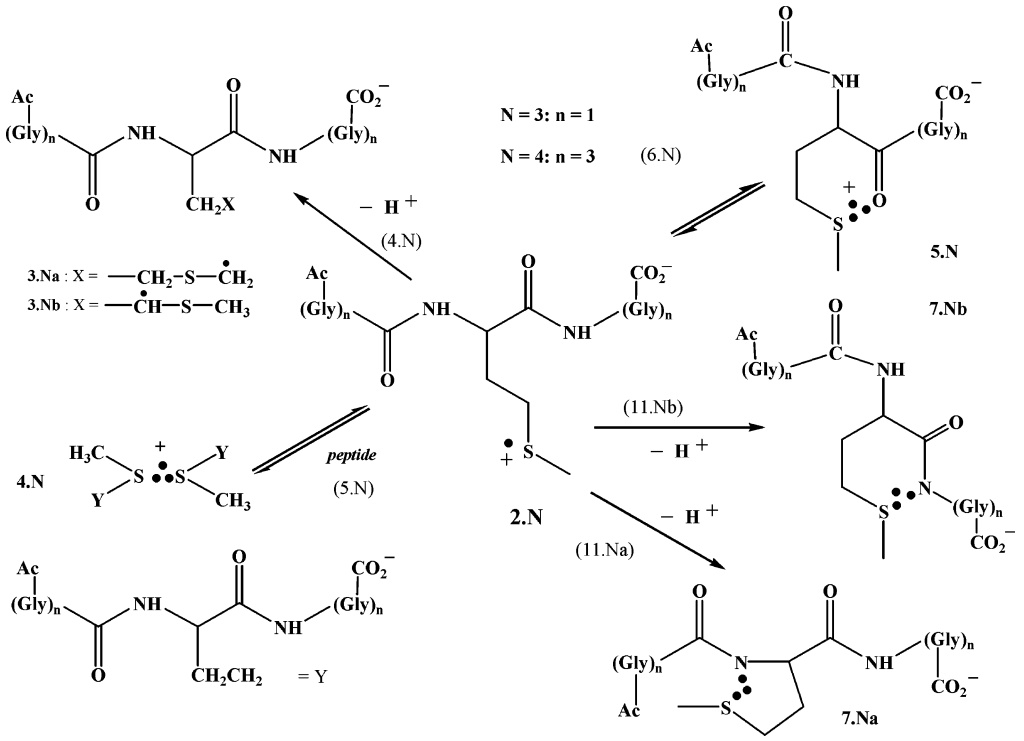

formation[52] yields $(G \times \Delta\Lambda)_{corr} = -190$ S cm^2. Division of $(G \times \Delta\Lambda)_{corr}$ by $\Delta\Lambda = -270$ S cm^2 equiv^{-1} yields G(ions) = 0.7, representing sulfide radical cations **4.3** and/or **5.3**.

Figures 9B shows the optical spectrum and its deconvolution taking into account species **3.3a**/**3.3b**, **4.3**, **5.3**, **6.3**, and **8** (Table S3, entry 5).

While the deconvolution results in a good fit of the experimental spectrum, the discrepancy between G(ions) = 0.7 (see above) and $G_{4.3+5.3} = 1.2$ is unacceptable. This mismatch is corrected by the additional inclusion of **7.3a/7.3b** in the deconvolution (Figure 9C; Table S3, entry 6). In this case, the agreement between G(ions) and $G_{4.2+5.3}$ is significantly improved. Without any doubt, the existence of the sulfur−nitrogen transient (**7.3a/7.3b**) is confirmed by applying complementary time-resolved conductivity and spectrophotometric measurements. At earlier time points after the pulse at this pH, conductivity measurements are more difficult to interpret quantitatively due to the slower neutralization reaction between H^+ and HO^-, formed in reactions 8 and 9. Hence, at these time points, a clear distinction between species **5.3** and **7.3a/7.3b** is impossible (Table S3, entries 1−4).

***N*-Ac-(Gly)$_3$Met(Gly)$_3$ (*N*-Ac-GGGMGGG).** Taking the published rate constant, k(•OH + *N*-AcGGG) = 2.4 × 10^9 M^{-1} s^{-1},[40] as a representative value for the reaction of •OH with *N*-Ac-GGGGGG,[61] and k(•OH + *N*-Ac-Met) = 6.7 × 10^9 M^{-1} s^{-1},[40] we would expect that ca. 25% of the initial •OH radicals directly abstract H-atoms from *N*-Ac-GGGMGGG. Figure 10 shows the optical spectrum recorded 20 μs after pulse irradiation of an N_2O-saturated aqueous solution of 2 × 10^{-4} M *N*-Ac-GGGMGGG at pH 5.3, together with the spectral deconvolution

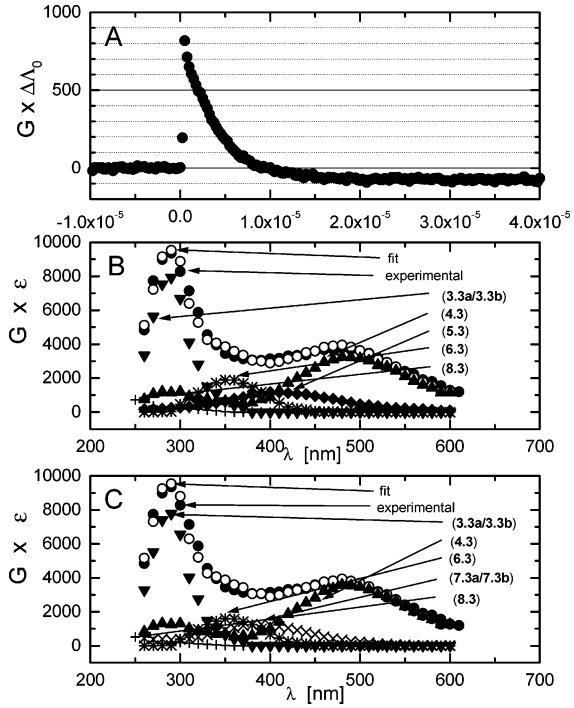

Figure 9. (A) Equivalent conductivity changes represented as $(G \times \Delta\Lambda)$ vs time profile following the •OH-induced oxidation of *N*-acetylglycyl-methionyl-glycine (2 × 10^{-4} M) in N_2O-saturated aqueous solutions at pH 5.45 (units of the *x*-axis: seconds); (B and C) resolution of the spectral components in the transient absorption spectrum following the •OH-induced oxidation of *N*-acetylglycyl-methionyl-glycine (2 × 10^{-4} M) in N_2O-saturated aqueous solutions at pH 5.45 taken 20 μs after the pulse (explanation in the text).

into contributions from species **3.4a/3.4b**, **4.4**, **5.4, 6.4**, **7.4a/7.4b**, and **8** (Table 4, entry 3). Based on G(ions) = $G_{4.4}$ = 0.5, we conclude that the only species absorbing around 390 nm is **7.4a/7.4b** and that **5.4** is not formed at this pH.

(61) By analogy to identical rate constants for the reaction of HO• radicals with *N*-Ac-(Ala)$_3$ and *N*-Ac-(Ala)$_6$.[40]
(62) Hawkins, C. L.; Davies, M. J. *J. Chem. Soc., Perkin Trans. 2* **1998**, 2617−2622.
(63) Hiller, K.-O.; Asmus, K.-D. *J. Phys. Chem.* **1983**, *87*, 3682−3688.

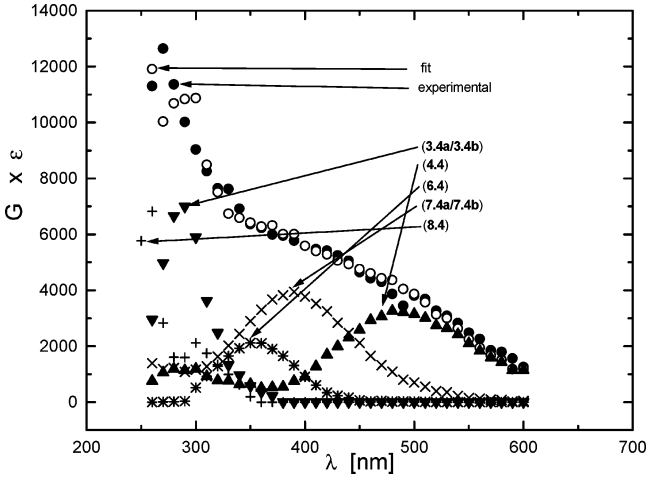

Figure 10. Resolution of the spectral components in the transient absorption spectrum following the •OH-induced oxidation of *N*-acetylglycyl-glycyl-glycyl-methionyl-glycyl-glycyl-glycine (2×10^{-4} M) in N_2O-saturated aqueous solutions at pH 5.3 taken 20 μs after the pulse.

The following features of these yields are important: we observe (i) substantially higher yields of glycyl radicals (**8**) in *N*-Ac-GGGMGGG compared to *N*-Ac-GMG; (ii) generally lower yields of **8** as predicted from the rate constants of HO• and H• with Gly and Met, respectively (vide supra); (iii) a preference for the intramolecular sulfur−nitrogen bonded transient (**7.Na/7.Nb**) over the intermolecular sulfur−sulfur transient (**4.N**) in *N*-Ac-GMG and *N*-AcGGGMGGG as the size of the model peptide increases (cf. $G_{\mathbf{7.Na/b}}/G_{\mathbf{4.N}} = 0.6$ for *N*-Ac-GMG and 1.8 for *N*-Ac-GGGMGGG at pH 5.3−5.4 at 20 μs after the pulse), and (iv) higher yields of C_α-centered radicals **6.N** for the peptides *N*-Ac-GMG (**6.3**) and *N*-AcGGGMGGG (**6.4**) in comparison to *N*-Ac-Met-NH_2 (**6.1**) and *N*-Ac-Met-OMe (**6.2**).

***N*-Acetylalanine Amide and Alanyl-alanine (*N*-Ac−Ala-NH_2 and Ala-Ala).** To obtain a reference spectrum for the C_α-substituted radical **6**, we pulse-irradiated N_2O-saturated aqueous solutions, pH 5.0, containing 2×10^{-4} M *N*-Ac-Ala-NH_2 or Ala-Ala. Both experiments gave transient spectra with an absorption peak at $\lambda_{max} = 350$ nm. For Ala-Ala, ESR experiments have yielded quantitative information about the relative reactivity of •OH radicals toward the individual C−H bonds, that is, ca. 67% with C_β−H and the remainder with Cb−H.[62] Of the 67% •OH attacking C_α−H, ca. half (i.e., a total of 33.5%) will react with the N-terminal and a second half with the C-terminal Ala residue. Reaction with the N-terminal Ala residue yields a radical of the type $H_2N-C^\bullet(CH_3)-CO-NH-R$ (**9**). Such α-amino-substituted radicals usually show structureless optical spectra with absorption maxima < 300 nm.[63] Therefore, the 350 nm absorbance derived from Ala-Ala is assigned to the C-terminal radical $R^1-CO-NH-C^\bullet(CH_3)-CO_2^-$ (**10**), which does not contain a free amino group. This assignment is supported by a similar spectrum obtained by pulse irradiation of *N*-Ac-Ala-NH_2.

Hence, the experimental spectrum derived from Ala-Ala is composed of contribution from radicals **9** and **10** with the spectrum of **10** being identical to that of **6**. Based on the known quantities of •OH forming **9** and **10**, and the known extinction coefficient for spectrum of **9**-type radicals, we extracted the spectrum for radical **10** with the following characteristics: $\lambda_{max} = 350$ nm and $\epsilon_{350} = 3150$ M^{-1} cm^{-1}. This spectrum is used for the quantification of **6**-type radicals in the deconvolutions of the optical data derived from *N*-Ac-Met-NH_2, *N*-Ac-Met-OMe, *N*-AcGMG, and *N*-Ac-GGGMGGG.

Discussion

Several observations are important for the interpretation of the results: (i) the yields of conductometrically quantified radical cations correspond well to the combined yields of S−S and S−O bonded intermediates **4.N** and **5.N**, respectively, whereas the S−N bonded species (**7.Na/7.Nb**) are not radical cations; (ii) ultimately, for all peptides most of the intermediates convert into α-(alkylthio)alkyl radicals **3.Na**/**3.Nb**; (iii) we do not observe any time-dependent formation of glycyl radicals (**8**) for *N*-Ac-GMG and *N*-Ac-GGGMGGG beyond yields, which are expected due to a direct attack of OH• and •H radicals at Gly residues.

Mechanism for the Formation of the S−N Bonded Species 7.Na/7.Nb. The reaction of •OH radicals with Met in peptides initially yields the hydroxysulfuranyl radical **1.N** which, at low peptide concentrations, decomposes via either direct elimination of OH^- (reaction 3.Na; Schemes 1 and 2) or a proton-assisted elimination of water (reaction 3.Nb; Schemes 1 and 2). While significant yields of **1.N** are detectable at 2 μs after the pulse, the decomposition of **1.N** is essentially completed within 6 μs after the pulse. This process leads to a very short-lived monomeric radical cation **2.N** which deprotonates irreversibly to **3.Na**/**3.Nb** (reaction 4.N) or associates either *inter*molecularly with a second peptide molecule (reaction 5.N) or *intra*molecularly with the amide or ester function within the peptide (reaction 6.N). In a neutral amide (−CO−NH−), the carbonyl oxygen represents the better nucleophile compared to the nitrogen,[64,65] so that the formation of an S−O bonded radical cation (reaction 6.N) is kinetically favorable compared to that of an S−N bonded radical. Our results corroborate this fact, showing mainly S−O but not S−N bonded intermediates for *N*-Ac-Met-NH_2 and *N*-Ac-Met-OMe at pH 4.0 and 4.6 and short time delays (2−3 μs after the pulse). Separate theoretical calculations show that these S−O bonds are electronically best described as two-center, three-electron (2s,1s*) bonds.[66]

For longer time delays and for pH > 4.6, this picture changes. For example, pulse irradiation of *N*-Ac-Met-NH_2 at pH 5.0 shows both S−O and S−N bonded species at 15 μs after the pulse. At pH 5.4, only the S−N but no S−O bonded intermediates were detected at 10 μs after the pulse. Hence, we propose that an initially formed S−O bonded radical cation can undergo an O-to-N migration following deprotonation of the amide nitrogen. Reactions 13a−15a (Scheme 4) and 13b−15b (Scheme 5) show these mechanisms representatively for C- and N-terminal amides of *N*-Ac-Met-NH_2, respectively.

Analogous processes have been reported for metal cations complexed to amides.[67] Initially, the sulfide radical cation **2.N** will form a bond with the amide carbonyl oxygen. Such complexation with a cation will change the pK_a of the amide nitrogen in structure **5.N**. For the complexation of divalent metals, amide pK_a values on the order of 3−4 (Pd^{II}) or 4−6

(64) Bruice, T. C.; Benkovic, S. *Bioorganic Mechanisms Vol. 1*; W. A. Benjamin, Inc.: New York, 1966; p 187.
(65) Rauk, A. *Orbital Interaction Theory of Organic Chemistry*; John Wiley & Sons: New York, 1994; p 148.
(66) Pogocki, D.; Serdiuk, K.; Schöneich, Ch. *J. Phys. Chem. A* **2003**, *107*, 7032−7042.
(67) Margerum, D. W.; Dukes, G. R. In *Metal Ions in Biological Systems*; Sigel, H., Ed.; Marecl Dekker: New York, 1974; Vol. 1, pp 157−212.

Scheme 4

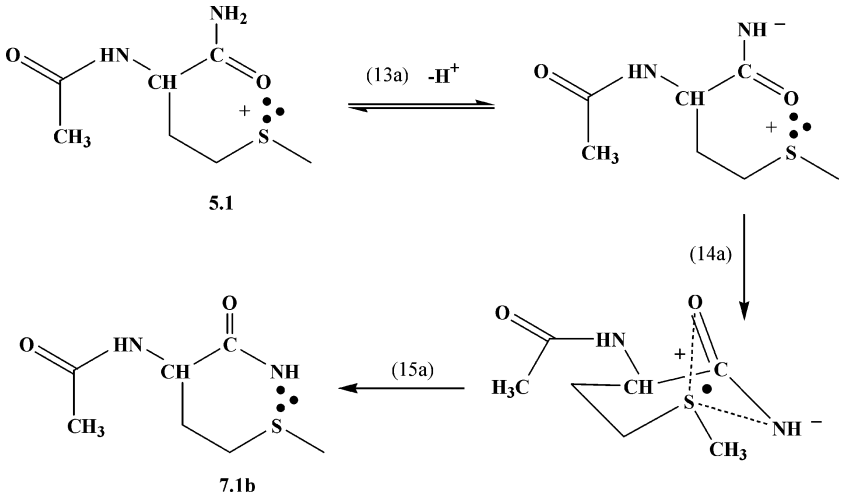

Scheme 5

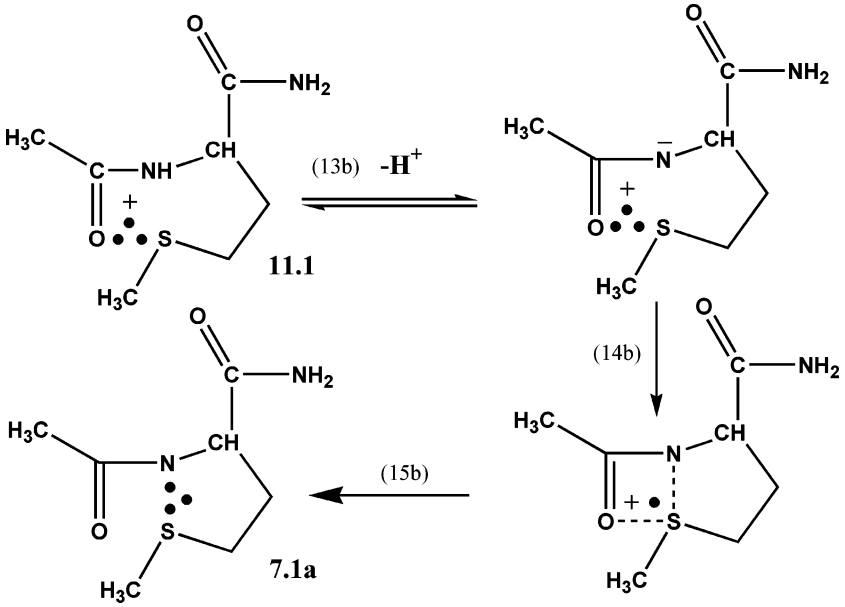

(Cu^{II}) have been observed,[67] suggesting that the "softer" metal ion causes the more acidic pK_a. Based on the trends in their association constants with several Lewis bases ($Cl^- < Br^- < I^-$),[68] organic sulfide radical cations can be considered "soft" Lewis acids and, therefore, through complexation, should be able to lower the pK_a of amides quite significantly. Therefore, we propose that the initial formation of S−O bonded species **5.N** may promote the deprotonation of the amide and subsequent reorientation into an S−N bonded overall neutral radical intermediate. In Schemes 4 and 5, the C-terminal S−O bond **5.1** converts into **7.1b**, and the N-terminal S−O bonded species **11.1**, into **7.1a**. Such a sequence of events is corroborated by our conductivity results, demonstrating that species **7.1a**/**7.1b** are not radical cations.

Three peptides in this study possess both a C- and an N-terminal amide, *N*-Ac-Met-NH_2, *N*-Ac-GMG, and *N*-Ac-GGGMGGG, whereas *N*-Ac-Met-OMe only possesses an N-terminal amide. The observation of S−N bonded species **7.2a** for *N*-Ac-Met-OMe confirms the possibility of reactions 13b−15b (Scheme 5) also for *N*-Ac-Met-NH_2.

Formation of the C_α-Radical 6.N. For all substrates, we detected the formation of C_α-radicals **6.N**. Importantly, they are observed specifically at higher pH arguing against a direct reaction of HO$^\bullet$ and H$^\bullet$ with the $^\alpha$C−H bond of Met as the source of **6.N**. We suggest that reactions 16−19 (Scheme 6) provide a facile route to radical **6.N**. In Scheme 6, ring opening of **7.Na** to the aminyl-type radical **12** (reaction 16), followed by an intramolecular 1,2-H-shift (reaction 17) represents an energetically less favorable pathway but has been included for completeness. Aminyl-type radicals react comparably to the isoelectronic alkoxyl radicals, for which solvent-assisted 1,2-H-shifts and α-β C−C fragmentation are common mechanisms: experimental evidence for a 1,2-H-shift (k ca. 10^3 s^{-1}) and α-β C−C fragmentation (k ca. 10^4−10^5 s^{-1}) was obtained for aminyl radicals from simple amino acids.[69−71] Hence, the protonation/deprotonation mechanism depicted in reactions 18b/19 provides an alternative to the intramolecular reaction 17 if

(68) Bonifacic, M.; Asmus, K.-D. *J. Chem. Soc., Perkin Trans. 2* **1980**, 758−762.

(69) Bonifacic, M.; Stefanic, I.; Hug, G. L.; Armstrong, D. A.; Asmus, K.-D. *J. Am. Chem. Soc.* **1998**, *120*, 9930−9940.

(70) Bonifacic, M.; Armstrong, D. A.; Carmichael, I.; Asmus, K.-D. *J. Phys. Chem. B* **2000**, *104*, 643−649.

(71) Wisniowski, P.; Carmichael, I.; Fessenden, R. W.; Hug, G. L. *J. Phys. Chem. A* **2002**, *106*, 4573−4580.

Scheme 6

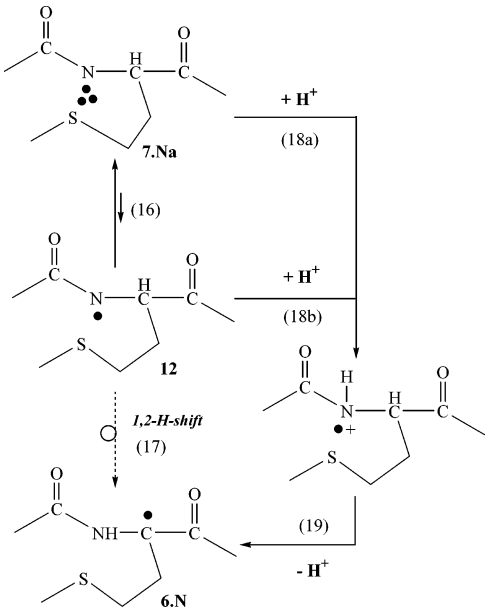

aminyl radical **12** was formed. The most probable pathway to radical **6.N** involves N-protonation of **7.Na**, followed by deprotonation at the $^{\alpha}$C-carbon (reactions 18a and 19). Reactions 16−19 provide an irreversible entry to carbon-centered radicals from Met in addition to reaction 4.N yielding the α-(alkylthio)-alkyl radicals **3.Na**/**3.Nb**. Together, **3.Na**/**3.Nb** and **6.N** represent the majority of carbon-centered radicals originating from the initial one-electron oxidation of the Met residue.

Met Sulfide Radical Cations Do Not Abstract H-Atoms from Gly in Linear Peptides. In a theoretical paper, Rauk et al.[37] have forwarded the hypothesis that Met sulfide radical cations in βAP, in the form of S−O bonded complexes formed with a neighboring carbonyl group, may abstract H-atoms from adjacent Gly residues in antiparallel β-sheet structures (reaction 20; Scheme 7), followed by deprotonation (reaction 21).

This hypothesis was based on the relatively low C−H bond dissociation energy (BDE) of Gly in antiparallel β-sheets (BDE ca. 361 kJ mol^{-1}) compared to other secondary structures, that is, BDE = 402 kJ mol^{-1} in the α-helix and BDE = 404 kJ mol^{-1} in the parallel β-sheet.[72] If this hypothesis is correct, Met sulfide radical cations should abstract H-atoms from Gly residues in linear, relaxed peptide structures where the Gly C−H bond has a BDE of 330−370 kJ mol^{-1},[72] which is similar or lower compared to the BDE of the Gly C−H bond in antiparallel β-sheets. One prerequisite for H-atom abstraction in both the antiparallel β-sheet and the linear peptides would be that the Met sulfide radical cation has access to the C−H bond in Gly during its lifetime. While at present no experimental data on antiparallel β-sheets exist, our data with linear peptides show that Met sulfide radical cations in their various S−O and S−N bonded complexes exist over several *microseconds* after pulse radiolytic formation. Moreover, our earlier experimental and computational studies show that even a short-lived ($t_{1/2}$ < 1 μs) S−O bonded sulfuranyl radical of Met in a linear peptide Thr-(Gly)$_n$-Met does interact unrestrictedly with up to five neighboring amino acid residues (i.e., n = 4) on the *nanosecond* time scale.[73] Hence, in the linear peptides *N*-Ac-GMG and *N*-Ac-GGGMGGG, we expect nearly unhindered access of any radical intermediate at the Met residue with one of the neighboring and highly flexible Gly residues during the lifetime of the radical intermediate. Experimentally, we do not observe any significant yields of glycyl radicals **8** beyond the yields expected from a direct reaction of •OH and •H with the Gly residues. Hence, the formation of glycyl radicals from any potential reaction of Met sulfide radical cations with neighboring Gly residues in linear peptides is of minor importance. This result underlines the importance of secondary structure for any potential H-transfer between Met sulfide radical cations and Gly. Unrestricted access of the reaction partners may not be sufficient: secondary structure, which not only allows collision of the reactants but also permits the maximal capto-dative stabilization of the forming radical **8** in the transition state will likely be an important parameter. An alternative route for the formation of glycyl radicals is H-transfer between Gly and the α-(alkylthio)alkyl radicals **3.Na/3.Nb** (or the peroxyl radical therefrom, formed after addition of molecular oxygen). These reactions are too slow to be followed on the pulse radiolysis time scale and need to be investigated by other experimental techniques.

Relevance to Redox Processes of Met^{35} in βAP. Several experiments document that Met^{35} in βAP is the source of the electron for the reduction of βAP-bound Cu^{II} to Cu^{I} (reaction 1). The ca. 1.0 V difference in the reduction and peak potentials of βAP-bound Cu^{II} and free Met, respectively,[21,29] suggest that equilibrium 1 is located far on the left-hand side. However, endergonic electron transfer processes are quite common when followed by strongly exergonic steps.[74] For example, the reduction of Ce^{IV} by *p*-xylene (reaction 22) occurs despite a potential difference of 1.0 V because the product *p*-xylene radical cation rapidly deprotonates with pK_a(ArCH$_3^{\bullet+}$) ≈ −6 (reaction 23).[75−77]

$$ArCH_3 + Ce^{IV} \rightarrow ArCH_3^{+\bullet} + Ce^{III} \qquad (22)$$

$$ArCH_3^{+\bullet} + B \rightarrow ArCH_2^{\bullet} + BH^{+} \qquad (23)$$

Theoretical calculations predict that pK_a(**2.N** → **3.Nb**) ≈ −6 and pK_a(**2.N** → **3.Na**) ≈ −2,[37] suggesting that the deprotonation of Met(S$^{+\bullet}$) alone (reaction 4.N) may drive equilibrium 1 toward the right-hand side comparable to the situation in the *p*-xylene/Ce^{IV} redox couple. In fact, our experiments indicate that carbon-centered radicals **3.Na**/**3.Nb** represent the predominant product radicals after the decay of S−S, S−O, and S−N bonded intermediates over longer time scales.

In addition, conformational properties of βAP promoting the stabilization of Met^{35} radical cations will play an important role in driving the one-electron reduction of Cu^{II}. In aqueous micelle solutions, NMR results indicate that the C-terminus of βAP1−40 is predominantly α-helical, that is, between residues Gln^{15} and Val^{36} with a kink or hinge around residues Gly^{25}-Asn^{27}.[78] The NMR studies on a truncated peptide in aqueous solution,

(72) Rauk, A.; Armstrong, D. A. *J. Am. Chem. Soc*. **2000**, *122*, 4185−4192.
(73) Pogocki, D.; Ghezzo-Schöneich, E.; Schöneich, Ch. *J. Phys. Chem. B* **2001**, *105*, 1250−1259.
(74) Eberson, L. *Electron-Transfer Reactions in Organic Chemistry*. Springer-Verlag: Heidelberg, 1987.
(75) Baciocchi, E.; Rol, C.; Mandolini, L. *J. Am. Chem. Soc*. **1980**, *102*, 7597−7598.
(76) Palombari, R.; Rol, C.; Sebastiani, G. *Gazz. Chim. Ital*. **1986**, *116*, 87.
(77) Schlesener, C. J.; Armatore, C.; Kochi, J. K. *J. Am. Chem. Soc*. **1984**, *106*, 3567−3577.
(78) Coles, M.; Bicknell, W.; Watson, A. A.; Fairlie, D. P.; Craik, D. J. *Biochemistry* **1998**, *37*, 11064−11077.

Scheme 7

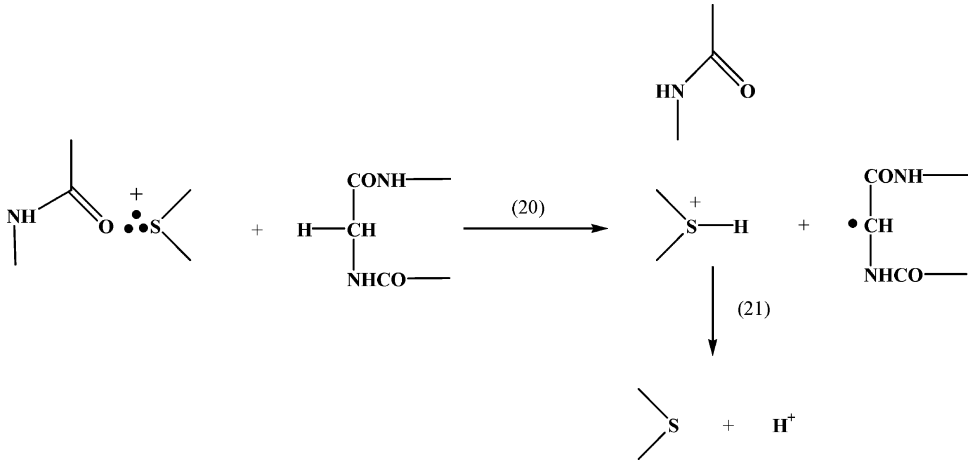

βAP10−35, indicate a collapsed coil structure.[79] However, CD studies on full length βAP1−42 document that the binding of Cu^{II} promotes a transition from low (8%) to high (57%) α-helix content.[21] Therefore, under conditions of electron transfer from Met to Cu^{II}, we can reasonably assume that the C-terminus of βAP is α-helical. In this α-helical conformation, the sulfur of Met^{35} is located at an average distance of ca. 3.6 Å from the carbonyl oxygen of the peptide bond C-terminal from Ile^{31}.[78] This distance is close to the sum of the van der Waals radii of sulfur and oxygen and suggests a preexisting S−O interaction. Such preexisting S−O interactions have been shown to promote the one-electron oxidation of sulfides in various model compounds,[80] and we hypothesize that the Ile^{31}-Met^{35} association will promote the one-electron oxidation of Met in βAP. The following support for this hypothesis has now been obtained. First, in molecular modeling calculations, we have shown that the one-electron oxidation of Met^{35} in βAP leads to S−O bond formation with the peptide bond C-terminal to Ile^{31} in an α-helical conformation.[32] If Ile^{31} is substituted by the helix-breaking residue Pro^{31}, the probability of S−O bond formation is significantly (ca. 90%) reduced.[32] Experimentally, we have then quantified the reduction of Cu^{II} for the mutant βAP1−42 (Ile^{31} → Pro^{31}), which is ca. 80% less effective compared to native βAP1−42.[81] Hence, the experimentally quantified reduction of Cu^{II} correlates well with the propensity of the Met^{35} sulfur to associate with the peptide bond C-terminal of amino acid residue 31.

In the current paper, we provide further experimental proof for the formation of S−O bonded radical cations after one-electron oxidation of Met in small peptides. Moreover, we show that such S−O bonded intermediates can deprotonate, followed by O-to-N migration of the sulfur, ultimately forming a neutral S−N bonded intermediate. Importantly, the ratio of such intramolecularly S−N bonded species versus intermolecularly S−S bonded species increases with increasing peptide size, suggesting that in a peptide as large as βAP the intramolecularly S−N bonded intermediate will be the dominant form of sulfur-centered radicals present. A fraction of the S−N bonded intermediate may suffer ring opening to yield a nitrogen-centered radical, which converts into a C_α-carbon radical (reactions 16−19). Additional yields of carbon-centered radicals are formed through reaction 4.N. Carbon-centered radicals are precursors for peroxyl radicals, which have been proposed as intermediates during the incubation of βAP in aqueous buffers based on ESR studies.[22] Our current experiments identify two possible structures of carbon-centered precursor radicals, which may be useful for the interpretation of ESR data obtained with βAP.

We find no experimental evidence for an H-transfer reaction between sulfide radical cations and Gly residues in linear model peptides. These findings do not exclude such H-transfer reactions in antiparallel β-sheets[37] but rather underline the importance for secondary structure for these reactions.

Undoubtedly, βAP ultimately aggregates to form β-sheets. However, recent experiments indicate that βAP reduces Cu^{II} most efficiently immediately after dissolution while the propensity to reduce Cu^{II} decreases significantly with prolonged incubation times (i.e., 24 h).[23] These data suggest that Cu^{II} reduction may not take place in large insoluble β-sheets but more likely in low molecular weight aggregates. The actual solution conformation(s) of the latter are unknown, but the CD data of Curtain et al.[21] suggest that they may initially contain a large proportion of α-helical structure. In an α-helical structure, the $^{\alpha}C-H$ BDEs of amino acids are high due to lower captodative stabilization of the product radical.[72] As a consequence, the formation of C_α-radical **6.N** could be slower in α-helices compared with random linear peptide sequences. On the other hand, the formation of C_α-radical **6.N** according to reaction 19 does not involve homolytic but heterolytic C−H bond breakage, for which no theoretical calculations are available.

Acknowledgment. The work described herein was supported by the NIH (PO1AG12993), SULFRAD (HPRN-CT-2002-00184), and the Office of Basic Energy Sciences of the U.S. Department of Energy. This paper is Document No. NDRL-4459 from the Notre Dame Radiation Laboratory.

Supporting Information Available: Selected radiation chemical yields (in terms of *G*-value) of all intermediates formed after pulse irradiation of aqueous solutions containing the following at various time delays: *N*-Ac-Met-NH_2, *N*-Ac-Met-OMe, *N*-Ac-Gly-Met-Gly (pH 5.45), and *N*-Ac-Gly-Gly-Gly-Met-Gly-Gly-Gly (pH 5.3).

JA036733B

(79) Zhang, S.; Iwata, K.; Lachenmann, M. J.; Peng, J. W.; Li, S.; Stimson, E. R.; Lu, Y.-A.; Felix, A. M.; Maggio, J. E.; Lee, J. P. *J. Struct. Biol.* **2000**, *130*, 130−141.
(80) Glass, R. S. In *Sulfur-Centered Reactive Intermediates in Chemistry and Biology*. Chatgilialoglu, C., Asmus, K.-D., Eds.; NATO ASI Series, Vol. 197; Plenum Press: New York, 1990; pp 213−226.
(81) Kanski, J.; Aksenova, M.; Schöneich, Ch.; Butterfield, D. A. *Free Radical Biol. Med.* **2002**, *32*, 1205−1211.